
Masters Theses

Student Theses and Dissertations

Fall 2017

Detection of mine roof failure using inexpensive LiDAR technology

Ali Abdullah M. Alzahrani

Follow this and additional works at: https://scholarsmine.mst.edu/masters_theses



Part of the [Geological Engineering Commons](#), and the [Mining Engineering Commons](#)

Department:

Recommended Citation

Alzahrani, Ali Abdullah M., "Detection of mine roof failure using inexpensive LiDAR technology" (2017).
Masters Theses. 7712.

https://scholarsmine.mst.edu/masters_theses/7712

This thesis is brought to you by Scholars' Mine, a service of the Missouri S&T Library and Learning Resources. This work is protected by U. S. Copyright Law. Unauthorized use including reproduction for redistribution requires the permission of the copyright holder. For more information, please contact scholarsmine@mst.edu.

**DETECTION OF MINE ROOF FAILURE USING INEXPENSIVE LIDAR
TECHNOLOGY**

by

ALI ABDULLAH M. ALZHRANI

A THESIS

Presented to the Faculty of the Graduate School of the

MISSOURI UNIVERSITY OF SCIENCE AND TECHNOLOGY

In Partial Fulfillment of the Requirements for the Degree

MASTER OF SCIENCE IN GEOLOGICAL ENGINEERING

2017

Approved By

Norbert H. Maerz, Advisor

Joe Guggenberger

Katherine Grote

© 2017

ALI ABDULLAH M. ALZHRANI

All Rights Reserved

ABSTRACT

Slope, Roof, and mine wall stability problems are some of the main reasons for deaths at U.S. surface or underground mining. The safety instruments were not enough to prevent that failure or even predict it before it occurs. However, the cost of such a tool that can be helpful in detecting roof failures is very high and not reachable in most instances.

The present study investigates the feasibility of using the M16 Leddar Evaluation Kit to detect the roof failure in mines. The M16 Leddar Evaluation kit cost is between 300\$-800\$, so it is the reachable price if it provides the required safety in mines. In fact, the underground mines have many openings, so the needs for instruments that can be distributed in all tunnels and safe all workers are urgent. The Leica Scan Station P40-3D Laser Scanner costs \$123915.00, so in mine industry, it is not worthy to establish the mining with such high cost like that. Buying one unit of the Leica ScanStation P40-3D Laser Scanner to provide the safety and minimize the expenses in the mining industry is not a practical idea which is providing safety to some of the workers in one tunnel spot and neglect the others.

Steel movement plate has been built and attached to a linear actuator that can move with a resolution around 0.00375 mm per step and stroke 50 mm in order to simulate the roof failures in mines. It is not possible to try the M16 in real mine due to the time limits and absence of not unstable mines locally, besides the intention that the author has to start with an office environment.

The M16 Leddar Evaluation kit is aimed directly to movement plate and collecting the deformation derived by the actuator. The results collected has many of anomalies and irregular data that can be eliminated by doing some of the statistical identification of outliers.

The results show that the M16 Leddar evaluation kit is capable of detecting the movement plate profile with a precision between 0.1 mm and 3 mm per integration period.

ACKNOWLEDGMENTS

The author is very indebted to Dr. Norbert Maerz. Without his guidance, support and good advice, it would not have been possible to finish this thesis without Dr. Norbert Maerz help and guidance. Dr. Maerz has opened the way in front of the way and lets the author expose his skills in various fields. Dr. Maerz has not ever hesitated to provide the author with any help. The author would like to thank Dr. Norbert Maerz who was a great professor who inspired the author with his deep knowledge and extended information in the field of Geological Engineering.

The author wants to thank my committee members for their patience, guidance and good humor: Dr. Joe Guggenberger as well as Dr. Katherine Grote.

As an international student, the author would like to say that it is not easy to accept the life in such different environment without the help and guidance of a close and kind people like Mr. Kenneth Boyoko and his wife, Marsha. Mr. Kenneth Boyoko taught the author the most important principles of Arduino programming plus Light Detection and Ranging principles.

The author is very grateful for his gorgeous supporting Family, who made the author the person whom he is today. Knowing that parents, sisters, and brothers are waiting for the author graduation is making all challenges to be a smaller till they fade away.

Most importantly, the author would like to express his profound thanks to his wife Budur who supports him in everything. Budur helped the author to get through two years of MST graduate school. Budur spent all day thinking how to simplify and organize the author schedule and keep the life excited and enjoyable even though in critical times or with challenging work. Budur taught the author how to enjoy the work and make a difference.

The only thing that the author can do to thank all people helped him in MST is to say, "I hope that I can do something in future that can pay back all helps I got from anybody."

TABLE OF CONTENTS

	Page
ABSTRACT.....	iii
ACKNOWLEDGMENTS	iv
LIST OF ILLUSTRATIONS.....	ix
LIST OF TABLES.....	xi
SECTION	
1 INTRODUCTION	1
1.1 ROCKFALLS IN MINES	1
1.2 THE FAILURE OF TECHNOLOGY TO REDUCE ROCKFALLS	6
1.3 CAUSES OF UNDERGROUND FAILURES.....	12
1.4 PRECURSOR MOVEMENT CAN BE USED IN PREDICTION FAILURE.....	12
1.5 TECHNOLOGICAL ADVANCES IN UNDERGROUND MONITORING.....	15
1.5.1 Introduction to the New Technological Advances.....	15
1.5.2 Total Station.....	15
1.5.2.1 Concept.	15
1.5.2.2 Components.	16
1.5.2.3 Installation.....	16
1.5.2.4 Advantages vs. disadvantages.....	16
1.5.2.5 Cost.	17
1.5.3 LIDAR.	17
1.5.3.1 Concept.	17
1.5.3.2 Components.	18
1.5.3.3 Installation.....	18
1.5.3.4 Advantages vs. disadvantages.....	18
1.5.3.5 Cost.	18
1.5.4 Extensometer.....	19
1.5.4.1 Concept.	19
1.5.4.2 Components.	19
1.5.4.3 Installation.....	19

1.5.4.4	Advantages and disadvantages.	19
1.5.4.5	Cost.	20
1.5.5	Photogrammetry.....	20
1.5.5.1	Concept.	20
1.5.5.2	Components.	21
1.5.5.3	Installation.....	21
1.5.5.4	Advantages and disadvantages.	21
1.5.5.5	Cost.	22
1.5.6	Seismic Monitoring System.....	22
1.5.6.1	Concept.	22
1.5.6.2	Components.	22
1.5.6.3	Installation.....	23
1.5.6.4	Advantages and disadvantages.	23
1.5.6.5	Cost.	23
2	USING LIDAR FOR MEASURING THE PRECURSOR MOVEMENTS	24
2.1	CAPABILITIES OF TERRESTRIAL LIDAR	24
2.2	USE OF INEXPENSIVELY FIXED LIDAR SCANNERS.....	28
3	PURPOSE OF THIS RESEARCH.....	31
4	RESEARCH TOOLS.....	32
4.1	DEVELOPMENT OF A ROCK DISPLACEMENT SIMULATOR (RDS).....	32
4.1.1	Introduction to the Rock Displacement Simulator (RDS).	32
4.1.2	Concept.	33
4.1.3	Components.	33
4.1.3.1	Target plate.	33
4.1.3.2	Linear actuator EZC4-05M (specifications).	36
4.1.3.3	Control circuit.	37
4.1.3.3.1	Introduction to the control circuit.	37
4.1.3.3.2	Stepper motor drivers.....	38
4.1.3.3.3	Trigger relay module.....	39
4.1.3.3.4	X-bees radio (transceiver).....	39
4.1.3.3.5	Arduino UNO microcontroller (MCU).	40

4.1.3.3.6	Liquid crystal display (LCD).....	40
4.1.3.3.7	Volts of direct current (VDC) power source.....	41
4.1.3.4	Software control.....	41
4.2	THE LINEAR ACTUATOR MODIFIED PRECISION CALCULATIONS	43
4.3	VERIFICATION.....	43
4.4	USING THE M16 SCANNER.....	45
4.4.1	Introduction to the M16 Scanner.	45
4.4.2	M16 Scanner and Software Developers.....	45
4.4.3	Properties and Standard Measurements of The M16.....	46
4.4.4	Scanning Protocol with The M16.	49
4.4.5	Capturing Raw M16 Measurements.	50
5	RECTIFYING M16 MEASUREMENTS	60
5.1	INTRODUCTION TO THE M16 MEASUREMENTS RECTIFICATION.....	60
5.2	PROBLEMS AND SOLUTIONS.....	61
5.2.1	Zero Offset Effect.	61
5.2.2	Environmental Variables Affecting the Scanning Results.	61
5.2.3	Drift Effect.....	61
5.2.4	M16 Settings Effect.	62
5.2.5	Segments Position Effects.....	62
5.2.6	Electrical Components Instability.....	63
5.2.7	M16 Internal Temperature Effect.	63
5.2.8	The Target Plate Material Effect.....	63
5.3	DATA RECTIFICATION TECHNIQUES	63
5.3.1	Introduction to the Rectification Techniques.....	63
5.3.2	IQR.....	64
5.3.3	Z-Score.....	65
5.3.4	Drift Correction.....	66
5.3.4.1	Dynamic segment NO. 9. (for detecting movements).	66
5.3.4.2	Static segment NO. 16. (for measuring the drift).....	66
5.3.5	Averaging.....	66
5.3.6	Moving Average.	67

6	DATA RESULTS, AND INTERPRETATION	69
6.1	STATIC TESTS AND RESULTS	69
6.2	RAW DATA OF THE STATIC TESTS VS. RECTIFIED DATA	69
6.3	DYNAMIC TESTS AND RESULTS	75
6.4	RAW DATA OF THE DYNAMIC TESTS VS. RECTIFIED DATA	81
7	CONCLUSIONS AND RECOMMENDATIONS	87
7.1	THESIS CONCLUSIONS	87
7.2	THESIS RECOMMENDATION.....	87
	BIBLIOGRAPHY.....	89
	VITA.....	94

LIST OF ILLUSTRATIONS

	Page
Figure 1.1: Roof failure due to horizontal stress.....	1
Figure 1.2: Large rock layer that has fallen inside a mine.....	3
Figure 1.3: Roof buckling and cutter roof due to horizontal stress	5
Figure 1.4: Number of fatalities in the USA since 1900 caused by roof buckling	7
Figure 1.5: Roof falls trend in an Illinois mine since 1983	7
Figure 1.6: The typical relationship between the stress and strain	13
Figure 1.7: The typical relationship between the strain and time	14
Figure 1.8: A total station or TST (Total Station Theodolite)	15
Figure 1.9: The Leica® scan station LIDAR.....	17
Figure 2.1: Terrestrial LIDAR	24
Figure 2.2: Dense 3D point cloud data collected by terrestrial LIDAR	27
Figure 4.1: The process of constructing the actuator frame.....	34
Figure 4.2: The welding process of the actuator frame	34
Figure 4.3: The final design of the actuator.....	35
Figure 4.4: Front view of the target plate	35
Figure 4.5: The EZ Limo EZC4-05M electromechanical linear actuator.....	36
Figure 4.6: Prototype of the programmable actuator circuit.....	38
Figure 4.7: Screenshot of the simulator program.....	41
Figure 4.8: One profile that has been used in the simulator program.....	42
Figure 4.9: The yellow target plate is moving toward the dial gauge.....	44
Figure 4.10: M16 scanner dimensions	46
Figure 4.11: Diagram shows one segment dimensions of the M16 sensor beam.....	47
Figure 4.12: The full beam measurements.....	48
Figure 4.13: M16 scanner power port +RS485.....	49
Figure 4.14: The waveform of the reflected energy from the target.....	53
Figure 4.15: Screenshot the main menu of configurator software.....	55
Figure 4.16: Illumination area and the detection zone.....	56
Figure 4.17: Raw detection available feature in the M16 software	57

Figure 4.18: The trigonometry calculation between the target and M16 scanner	58
Figure 5.1: All 16 segments aimed at the same planar target	62
Figure 5.2: Interquartile range box and whiskers plot	64
Figure 5.3: The z-score used to cut off the tails of the distance collected data	65
Figure 5.4: Forward moving average.....	68
Figure 5.5: Backward moving average	68
Figure 6.1: Raw data of the static test NO. 1.....	70
Figure 6.2: Rectified data of the static test NO. 1.....	71
Figure 6.3: Raw data of the static test NO. 2.....	72
Figure 6.4: Rectified data of the static test NO. 2.....	73
Figure 6.5: Raw data of the static test NO. 3.....	74
Figure 6.6: Rectified data of the static test NO. 3.....	75
Figure 6.7: Actuator profile NO. 1.....	76
Figure 6.8: Actuator profile NO. 2.....	77
Figure 6.9: Actuator profile NO. 3.....	78
Figure 6.10: To detect the target plate accurately, the M16 scanner light beam	80
Figure 6.11: Raw data of the dynamic test NO. 1.....	81
Figure 6.12: Rectified data of the dynamic test NO. 1	82
Figure 6.13: Raw data of the dynamic test NO. 2.....	83
Figure 6.14: Rectified data of the dynamic test NO. 2	83
Figure 6.15: Raw data of the dynamic test NO. 3.....	85
Figure 6.16: Rectified data of the dynamic test NO. 3	85

LIST OF TABLES

	Page
Table 1.1: All mine accidents in the USA with five or more fatalities, since 1970	4
Table 4.1: Terminal block connector pin definition	50
Table 4.2: The measurement rate of the configurator software	52
Table 4.3: Field description of the log text file.....	59
Table 5.1: The test NO. versus test type (Dynamic/Static).....	60
Table 6.1: The maximum drift of raw data of the static test NO. 1	70
Table 6.2: The maximum drift of rectified data of the static test NO. 1.....	71
Table 6.3: The maximum drift of raw data of the static test NO. 2	72
Table 6.4: The maximum drift of rectified data of the static test NO. 2.....	73
Table 6.5: The maximum drift of raw data of the static test NO. 3	74
Table 6.6: The maximum drift of rectified data of the static test NO. 3.....	75
Table 6.7: Actuator profile NO. 1	76
Table 6.8: Actuator profile NO. 2.....	77
Table 6.9: Actuator profile NO. 3.....	78
Table 6.10: Scan duration and maximum movement of every single test	79
Table 6.11: Actuator vs. the detected profile the rectified dynamic test NO. 1 data.	82
Table 6.12: Actuator vs. the detected profile of the rectified dynamic test NO. 2 data....	84
Table 6.13: Actuator vs. the detected profile of the rectified dynamic test NO. 3 data....	86

1 INTRODUCTION

1.1 ROCKFALLS IN MINES

Slope, roof, and mine wall stability problems are some of the main reasons for deaths at U.S. surface or underground mines (Figure 1.1). Two West Virginia miners in Brody mine were killed recently in a coal mine due to a wall collapse at the mine which is owned by Patriot Coal (Spencer 2014).

The federal safety authorities had put the Brody Mine under greater scrutiny, but the failure occurred regardless. It is important to have all safety requirements in all mines to preserve the lives of those workers inside the mine.

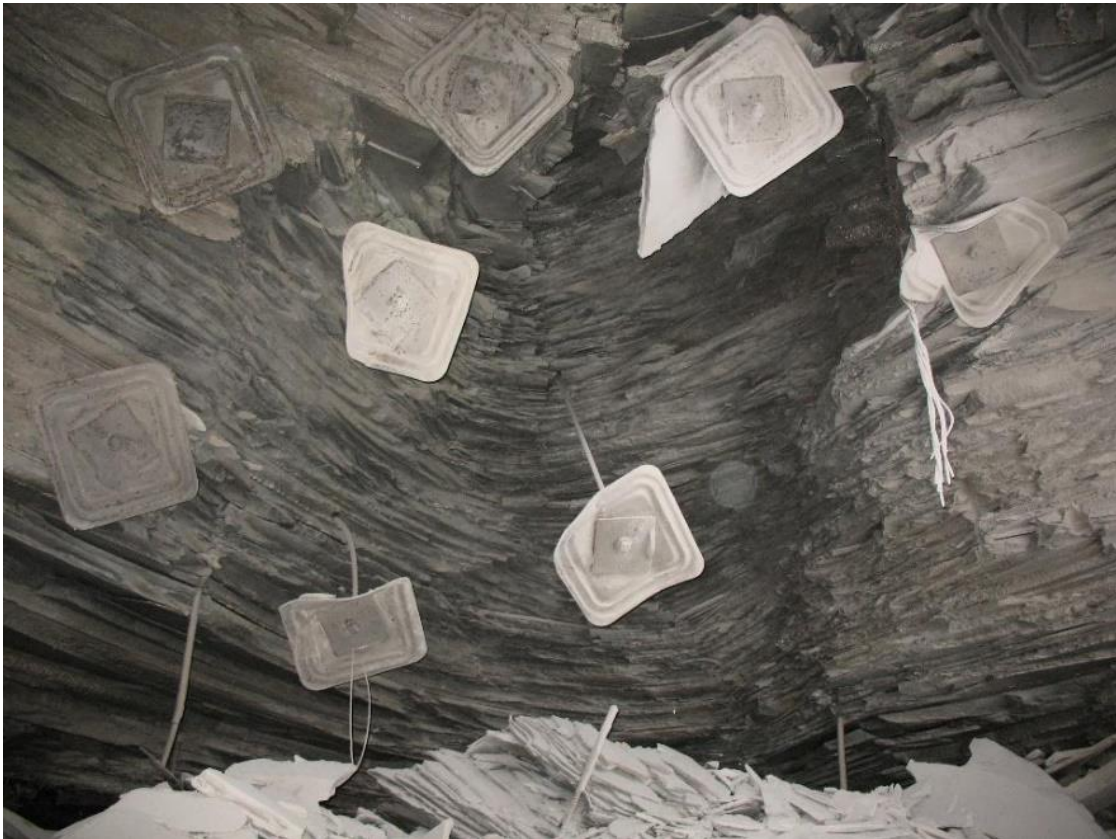


Figure 1.1: Roof failure due to horizontal stress.

The mining industry is maturing, so that will increase the demand for expertise in the mining field. Thus, a large number of people will be affected by the hazardous situations while working in a mine.

With even more people participating in the mining industry the need for strict requirements of safe mining practices and environments also increases.

Rock masses movement cannot be predicted in all instances. It is impossible to detect all rockfall hazards before they occur.

Some risks are obvious, and some others are not such as large boulders at the edge of a rock mass, are obvious, but others which appear to be part of a solid rock face are slowly released until a small block falls, causing a cascading failure.

The release of some of the smaller blocks may cause a chain reaction creating more rockfall or in some instances large-scale rock failure (Hoek 2000).

There is no perfect solution to any problem especially when it has many compounding parameters such as in the mines roof failures. However, it is important to plan and design for the highest safety level in the mining industry.

This thesis will focus on one point which might prove to be a great hope in detecting roof movement and generating warning notifications to the workers thru an integrated system consisting of radio nodes, microcontrollers, and a LED sensor which will be responsible for detecting the ground movement.

The components of the LED sensor, microcontroller, and radio nodes are connected to a laptop computer to store the measured data, and it is possible to link that laptop by web protocols to make the connection with the sensor(s) inside the mine and its data available from anywhere and anytime.

The system will be designed to increase mine safety and to minimize the number of incidents, injuries, deaths, and significant economic loss.

The roof failure problem can be severe due to the fall of massive layers of rock (Figure 1.2), or the fall of smaller broken blocks, and as such it should be taken seriously by developing new tools such as monitoring instruments and alarm systems which can detect the precursor movements before it fails catastrophically.

Thus, the workers will have enough time after getting the alarm to move away from the fall area and protect themselves.

Table (1.1) recounts the amount of suffering and loss which has happened in some mines. More importantly, having an alarm system just in case was not enough in preserving the workers inside.

There are three reasons for all ground failures in all mine safety and health administration (MSHA) ground fall fatality reports between 1999 and 2008.



Figure 1.2: Large rock layer that has fallen inside a mine (Molinda and Mark 2010).

The first reason is the pillar failure which was the main principal reason of ground fall fatalities by (19%) overall ground fall fatalities. The next two reasons respectively are the rib failure and roof failure by (16% each) (Pappas and Mark 2012).

All underground mines could be subjected to the ground failures. As a result, more than 90% of the more than 700 underground mines use several types of roof/rib support.

Table 1.1: All mine accidents in the USA with five or more fatalities, since 1970 (Bajpayee, Pappas, and Ellenberger 2014).

Year	Mine	Location	Deaths
2010	Upper Branch, Performance Coal Co.	Raleigh County, W Virginia	29
2007	Crandall Canyon, Genwal Inc.	Emery County, Utah	6
2001	NO. 5 Mine, Jim Walter Resources Co.	Tuscaloosa County, Alabama	13
1986	Loveridge 22, Consolidation Coal Co.	Marion Co., West Virginia	5
1984	Wilberg Mine, Emery Mining Corp.	Emery Co., Utah	27
1983	McClure 1 Mine, Clinchfield Coal Co.	Dickinson Co., Virginia	7
1980	Ferrell NO. 17, Westmorland Coal Co.	Boone Co., West Virginia	5
1978	Moss NO.3 A, Clinchfield Coal Co.	Dickinson Co., Virginia	5
1977	Porter Tunnel, Kocher Coal Co.	Schuylkill Co., Pennsylvania	9
1976	Scotia Mine, Blue Diamond Coal Co.	Letcher Co., Kentucky	26
1972	Itmann NO. 3 Mine, Itmann Coal Co.	Wyoming Co., W Virginia	5
1972	Blacksville NO. 1, Consolidation Coal	Monongalia Co., W. Virginia	9
1970	Nos. 15, 16 Mines, Finley Coal	Leslie Co., Kentucky	38

Therefore, ground falls represent a significant risk to undergrounds mine miners. The appropriate supporting selection and adequate support system design are critical to the prevention of the ground failures and ground fall incidents. Also, there are nearly 2,000 reportable non-injury ground falls (Figure 1.3).

One of the biggest disasters in 2010 happened in a coal mine in Raleigh County, Montcoal, West Virginia causing 29 deaths (Srivastava, Ranjan, and others 2010). The roof fall count remained partially consistent with the study period, between 979 and 1,363 per year, the resultant average per year is 1160 falls.

So, the problem is responsible for many deaths in the mining industry. It is very important to investigate the problem seriously. (Figure 1.3) shows the approximate annually non-injury roof failures (about 11,600 non-injury roof falls between 1999 through 2008).

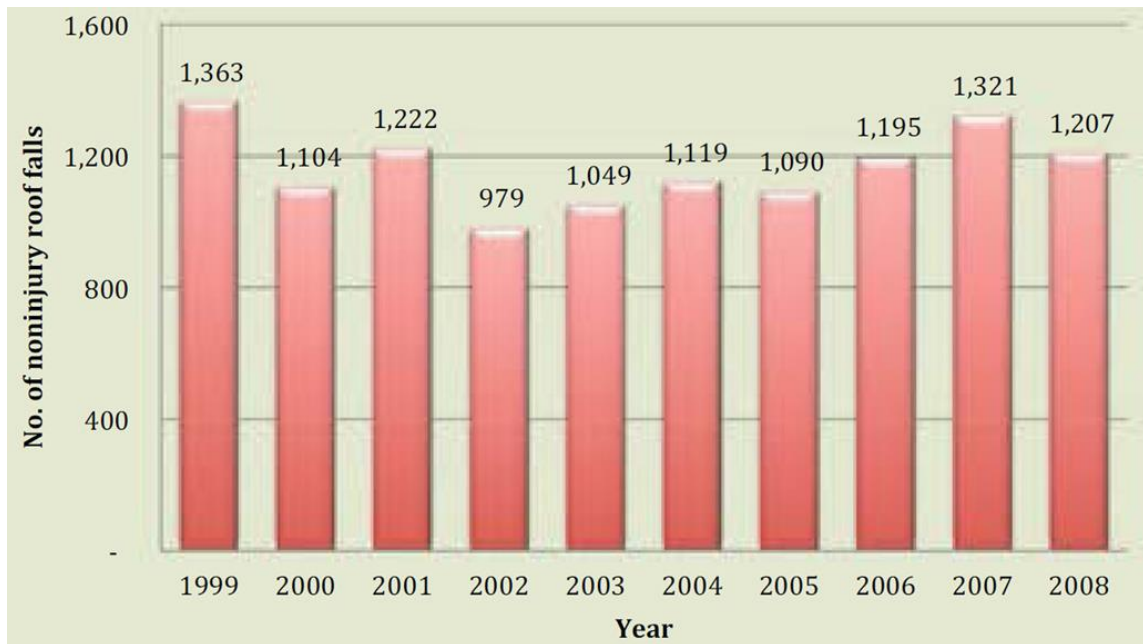


Figure 1.3: Roof buckling and cutter roof due to horizontal stress (Bajpayee, Pappas, and Ellenberger 2014).

Ground fall accidents in underground mines cause 8 to 10 deaths and more than 800 injuries per year. This represents approximately 30% of the fatal incidents and 15% of the injuries that occur every year in the subsurface mines. In addition, there are about 2,000 reportable non-injury ground failures.

1.2 THE FAILURE OF TECHNOLOGY TO REDUCE ROCKFALLS

The necessity of developing a methodology for reducing risk in the mines has had a remarkable role in the safety of industrial mining field.

In this thesis, a brief description of the most dangerous problems in the industrial mining field will be given, and afterward a detailed information about the suggested system which can help to avoid the risk region or evacuate the mine when it is needed.

It is noteworthy that the numbers of the mine ceiling failure which occurred in the past are still increasing which means roof failures may not have been prevented by any of the innovations or technologies which have been developed in this century.

The development of technologies that can at least alarm the workers in case of the possible failure in mines is very substantial.

The number of fatalities and incidents are less in the last 40 years if compared to 100 years ago. In fact, the most important aspect is to look at is the last 40 years which are the years that produced a lot of innovations and modern technologies.

Unfortunately, these technologies and innovation did not change the unfortunate situation caused by mine disasters. It is evident to see that from 1975 until now the rate of mine fatalities is still the same (Figure 1.4).

(Figure 1.4) shows the mining disaster accidents and deaths between 1900 through 2015. A mining disaster is an accident with 5 or more deaths. During the period, 591 mining disaster incidents were resulting in 12,800 fatalities.

One of the case studies in an Illinois mine shows that the roof failures are increasing over time even within the supported mine due to the deterioration of the rock between the rock bolts (Figure 1.5).

Reducing risk inside the mine and maximizing safety are the most important things that can be done for the miners. In general, the rock falls are caused by numerous disturbance factors, and it is not possible to prevent all of the failures.

Through the global awareness and extensive work, it is possible to mitigate or reduce the rockfalls.

It is reasonable to alleviate (mitigate) the rock falls by considering the most important factors including the knowledge about the rock falls, economy, time, and redundancy.

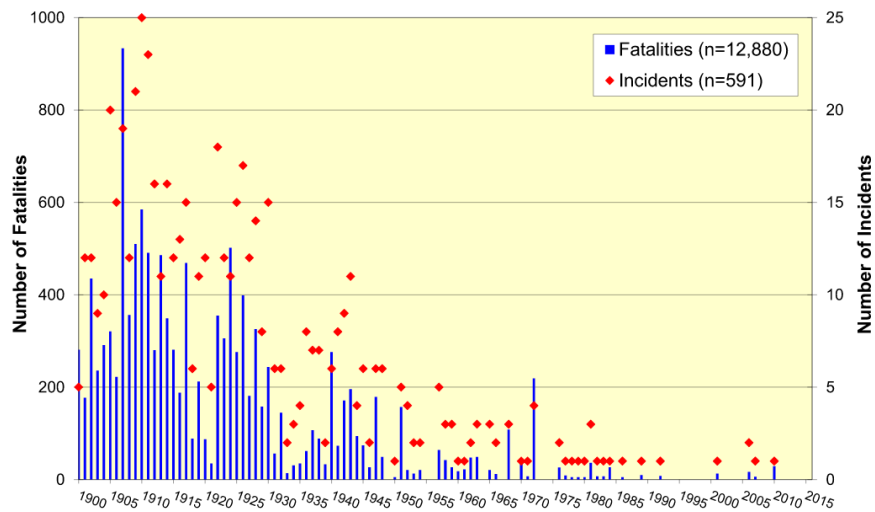


Figure 1.4: Number of fatalities in the USA since 1900 caused by roof buckling (Bajpayee, Pappas, and Ellenberger 2014).

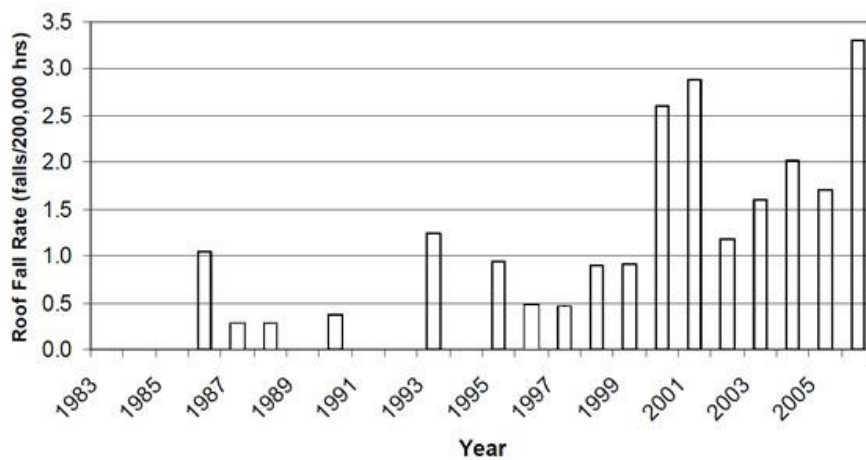


Figure 1.5: Roof falls trend in an Illinois mine since 1983 (Molinda and Mark 2010).

Reducing risk inside the mine and maximizing safety are the principal things to improve the outlook of the miners. Currently, with the increase of automation in the mine, it is easier to work with electronic tools that carry out many of the time-consuming and possibly dangerous tasks miners faced every day. However any solution has advantages and disadvantages, so it is important to understand the four things below which they are very important to make the solution of the roof failure problem in underground mines global and useful. The intuitive reasons that make solutions to the roof failure and perhaps to most of the engineering problems highly useful are:

- ❖ The solution is simple or easy to work.
- ❖ It is not time-consuming.
- ❖ It is not expensive to acquire, operate, and maintain.
- ❖ It can efficiently provide for safety.

In some instances, it is urgent for the operator to have real-time results that can be used as a trigger for sounding alarms. One of the recent technologies that are being used in industrial mining field is the light detection and ranging (LIDAR) scanning technology.

It is well-known technology that can detect very small movements. MoDOT initiated a research project to compare between various available LIDAR tools (Organizational Results Division 2011).

The aim of this project is to demonstrate the use and document the advantages and disadvantages of the rock fall data being collected from the inexpensive LIDAR in this thesis versus the most popular tools depending on the following:

- ❖ The capital cost of the equipment.
- ❖ The operating cost of the equipment and data interpretation.
- ❖ The time required for measurements.
- ❖ The safety of using the tool.
- ❖ The data quality being collected (the accuracy of the collected data).

In some instances, it is necessary for the operator to have real-time results that can be used as a trigger for the alarm system. Unfortunately, this kind of technology is hard to obtain under current mining conditions, because most existing technologies have some delays in communication, sometimes very significant. Regarding the failure of the

technology to mitigate the failures, it is not possible to ignore the cost of modern technologies that have been used to reduce the rockfalls or predict the failure before the occurrence.

The costs are a real factor in management decision making. The cost is a fundamental element in making some hard decisions such as spending several thousand dollars to have a low performing safety system or vice versa.

For the sake of the people lives, their future is what matters, not the cost, but it would be an easy decision in the case of a low-cost, high-performance safety system. The standard system in monitoring the rock failures uses the total station technology which sends a beam of light to one or more preplaced targets. However, it is not capable of detecting across a larger extent of rock unless many targets are installed.

In fact, the total station and the other light-based technologies are not capable of monitoring approximately more than 100 meters range (Addison and Gaiani 2000) with accuracy better than 1 mm. The most of the rock failure precursor movements are much smaller than the mentioned accuracy even though the laser technology being used to monitor the rock movement widely. The light-based technologies still imperative to put the cost into consideration besides the range, and the limitation of the beam light.

There are additional types of problems faced by workers in the mines working environment. In the following paragraphs list some problems that technologies could not easily solve:

- ❖ Communication problems in wired or even wireless communication technology that is used for sending the monitoring signals over long distances through the mine openings or the layers of the earth. Radio signals typically are blocked by the rock pillars, rock masses, or any other material kind that could insulate the signals. Wired transmissions depend on signals that were driven through cables that are expensive to install, prone to damage by excavation, extraction, roof collapse, or by carelessness by equipment operators.
- ❖ Traditional ground based LIDAR scanners have the issue of the cost to buy or even just to operate. It is hard to justify the cost for a mine for which the cost of monitoring will be a significant percentage of the operating cost.

The main purpose of the technology is used to keep the mine personnel away from the risk area in the situation of an imminent failure. In mine roof failures, the risk mitigation must often encounter hurdles related to economic resources, some environmental impact, and some logistic problems.

The previous requirements are critical; if any component fails, the whole series will fail also. Lack of accurate monitoring and detecting can be a reason for a missing rock fall event or conversely, it can also produce a false alarm and the subsequent loss of confidence in the used system. Any monitoring system should include the following (DiBiagio and Kjekstad 2007):

- ❖ Monitoring, including the data acquisition stage, transmission stage, and finally the maintenance of the instruments.
- ❖ Processing and predicting by the thresholds use, an expert judgment to the detected data can be one possible solution or even some other techniques such as the forecasting methods.
- ❖ Warning and the immediate alarm circulation.
- ❖ A response should be taken after getting the alarm.

The risk evaluation can be the first fundamental step for the design of every monitoring system depending on the geological and geomechanical knowledge is to determine the most critical parameters to be monitored (IEWP 2008).

A sophisticated system which is difficult to use or learn is one of the strong reasons for technology failures in reducing the rockfall problem. The production work of the mineral resources must be continuous while the safety of the workers and the equipment must be protected as much as possible.

The threshold alarm that is very conservative may lead to numerous false alarms and in indirect significant economic losses, whereas the high threshold alarm that is not conservative could put the mines or any other workers around the rock falls at risk in the situation of a missed alarm (Gigli et al. 2011).

The following points highlight various specific requirements and other practical issues that would have to be taken into the consideration when designing any rock falls monitoring, detection, and prediction system (Michoud et al. 2013):

- ❖ Pre-investigations should be done to evaluate the risk and provide a better understanding of the ground conditions.
- ❖ Redundancy, simplicity, robustness in communication and power supply backups are necessary for a reliable monitoring system besides supporting a near real-time reporting of the stability conditions.
- ❖ The alert levels are critical and should be based on the reliable energy response models only, and consequently, the alerts should be sent out as fast as possible.
- ❖ The awareness should extend to the highest levels in a mining organization, with extensive plans for appropriate behavior of workers in the case of alarm.

The detection and prediction technologies are limited by some of the theoretical and practical issues as follows:

- ❖ The difficulties related to the installation and maintenance of the sensor.
- ❖ The challenges related to the data transmission which should be at least near real-time integration of detected data while some of the modern technologies have some delays in transmitting the data (Bichler et al. 2004).
- ❖ The difficulties related to the hydrology factors, since the water is involved in about 86% of the rock masses destabilizations (Michoud et al. 2013). If the hydrology factors impact and destabilize the rock masses, it should also naturally impact the roof in mines.
- ❖ The last difficulty is the procedures to develop and improve the reliability and the pertinence in the automatic alarms (Michoud et al. 2013).

The next question in rockfall monitoring systems and that has to be answered: how to go from the expensive and complex monitoring system to easy and inexpensive surveillance systems (Troisi and Negro 2013).

1.3 CAUSES OF UNDERGROUND FAILURES

It is often difficult to understand the specific reasons for a roof failure (Smith 1984). Also, it is not always easy to determine or measure the factors which contribute to the mine ceiling failure in most instances, but here some of the factors which might be main reasons for the mine ceiling failure: As Smith (1984) said that all roof failures could be traced to two major causes:

- ❖ The interference of stresses in the roof of the mine, pillars, and floor exceeded the strength of the rock.
- ❖ Geological Factors, such as:
 - a) Rock type, Slickensides, and thickness of the strata.
 - b) Fractures in the roof, and the presence of water.
 - c) The presence of discontinuities, joints, and fractures.

In general, Dougherty (1971) discovered that roof failure in coal mines varies from rock type to another. The roof failure in sandstone occurred 7% of all incidents, and 12% of the time, if the rock type was coal, while 80% of roof falls took place when the roof consisted of unprotected shales (Dougherty 1971). So, after all of the research and analytical work that it has been done, it is intuitive to say that the roof failure has been attributed to be one of the biggest factors of death in underground mines. It is important to understand that the accumulating of all deaths in coal mines has gone over 50% in the United States coal mines (Peng 1978).

1.4 PRECURSOR MOVEMENT CAN BE USED IN PREDICTION FAILURE

Rock masses have various rock fall mechanisms the understanding of which can be exploited in such a way to monitor, detect and predict the failure. These rock fall mechanisms in mines can be classified into six points (Shen, King, and Guo 2007):

- ❖ Beam type of failure: beam failure often occurs in bedded rock roofs.
- ❖ Joint control rock falls: This mechanism of the rock failures often takes place in hard rock roof where joints are well developed.
- ❖ Roof sag: often present in the soft rock in deep underground mines. High stress and low rock strength lead to significant plastic displacement.

- ❖ Guttering and shear failure: One of the common failure mechanism in Australian underground coal mines.
- ❖ Skin failure: Small failure takes place in the unsupported laminated roof.
- ❖ Rib spalling/failure: Rib splitting is the inability of the roadway rock masses.

Different modes of failure occur in mining workings. In fact, three principal types of displacement can be used to track the unstable regions; any possible failure could begin with one of the following mechanisms:

- ❖ Initial response: after excavation, the period of initial reaction is a result of the elastic rebound or relaxation of stress (Zavis M , Zavodni 2000).
- ❖ Regressive/Progressive Deformation: the next stage directly after the initial deformation (Wyllie and Mah 2004).
- ❖ Long-term creep: long-term creep may happen where there is no determined failure surface, but its occurrence is due to stress relief (Wyllie and Mah 2004).

In plotting the stress versus the strain output data of the failure of a typical rock, the expected result should be as shown in (Figure 1.6).

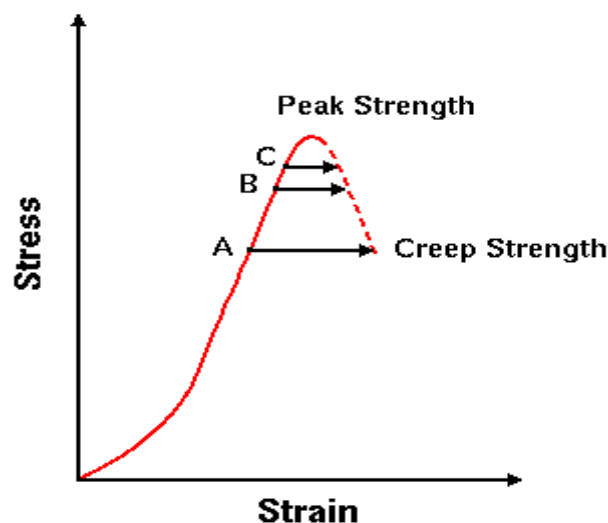


Figure 1.6: The typical relationship between the stress and strain.

The axial force on a rock core specimen should increase in a logical direction with the strain amount till the rock sample breaks. The rock sample deforms during this process until failure.

The constant stress is driving the sample to creep and move toward the point of the maximum/peak strength. This process of the time-dependent displacement under constant stress is well-known behavior in any rock stress-strain relationship.

The brief description of the strain and the time relationship (Figure 1.7) is as follows: First: the strain gradually increases proportional to the stress, as time passes under stress, the strain rate of reduces. This period of slowing-strain-rate is named primary behavior.

The first behavior stage is followed by an extended stage of slow (in general steady) displacement behavior. The last stage, the strain-rate starts to accelerate, to rapid and catastrophic failure.

The final stage of the fast displacement is named tertiary behavior. During the first two stages, it is possible (depending on the length of time) to monitor and detect the creeping movement of the rock mass.

The major time window while the failure is within the primary and secondary phase, could be used to monitor the movement and to alarm the workers if such movements occur.

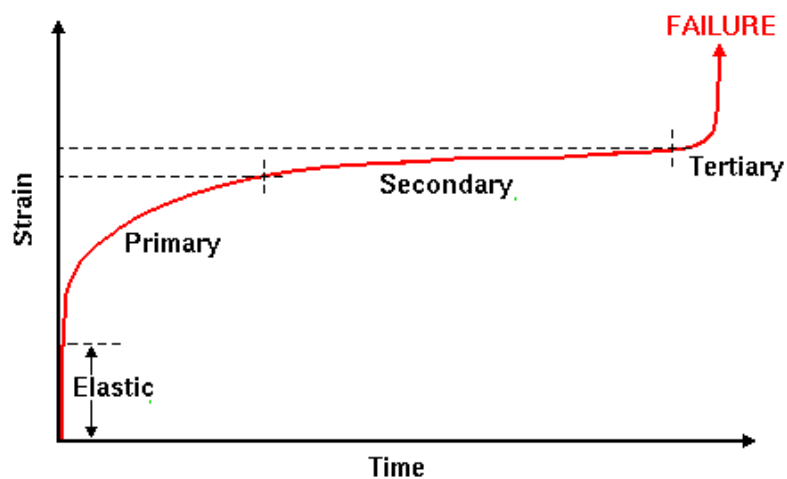


Figure 1.7: The typical relationship between the strain and time.

1.5 TECHNOLOGICAL ADVANCES IN UNDERGROUND MONITORING

These new technological advances in underground monitoring systems are used to monitor the displacement within the walls or roofs in mines.

1.5.1 Introduction to the New Technological Advances. Radar, extensometers, and surveying monitoring systems have been utilized in mines since the 1990s. These systems are used to monitor displacement within the walls or roofs in mines. The information collected can be used to forecast events such as rock falls and to help to keep miners safe. After determining the amount of movement, the rate of displacement can be tracked and used to predict the failure. There are conventional instruments that can be used to monitor and detect the rock deformation in mines as follows:

1.5.2 Total Station. This technique is broken down into 5 points.

1.5.2.1 Concept. A total station (Figure 1.8) is an optical instrument which is used in building and construction. A total station has the ability to collect the data through its electronic theodolite regarding distances and angles between the instrument and target points. This device is reliable for mining since it measures elevations, horizontal, and vertical angles. A total station machine is a primary tool for surveying and monitoring in the mining field. Surveyors usually use total stations to record tunnel ceilings, tunnel walls, and floors (Uren and Price 2010). The collected data gets stored in a Computer Aided Design (CAD) software for comparison with the created tunnel pre-design.



Figure 1.8: A total station or TST (Total Station Theodolite). The (TST) is an electronic/optical instrument used in modern surveying and building construction (Leica Geosystems 2012).

1.5.2.2 Components. A total station is characterized by four main components which entail; the electronic theodolite, electronic distance measurement (EDM), electronic display, and a microprocessor. The EDM has the main task of measuring the distance from the total station device to a reflector using electromagnetic energy to determine a line's length. The theodolite measures both vertical and horizontal angles.

The standalone theodolite combines level bubble, optical plummet, and calibrated circles to identify the required angles (Milsom and Eriksen 2011). The microprocessor has numerous tasks such as calculating averages of multiple angle measurements, vertical and horizontal distances, inverses, as well as the coordinates of X, Y, and Z. Lastly, the electronic display brings forth visuals of the activities taking place in the entire total station.

1.5.2.3 Installation. The installation (setup) of total stations in an underground mine starts by extending its three tripod legs to the required height, tightening the knobs, and opening the legs in a triangular manner. The next step entails placing the instrument on the tripod and securing it with a tripod screw. The surveyor is then required to press the legs into the ground for stability, after which individual legs are either lowered or raised for purposes of leveling the mount. This task leads to the installation of target prisms, a task while paves the way for fine-tuning. A reflector target/reflectorless should be positioned in the desired place is required to use the total station machine.

By using the focus feature on the lens to make sure a clear and focused view of the reflector target and that the cross-shaped hairs are centered on the center of the reflector (Olsen, Raugust, and Roe 2013).

1.5.2.4 Advantages vs. disadvantages. A total station is advantageous in that it is characterized by a quick setup on the tripod by using the laser plummet. This aspect makes it usable by professionals from different backgrounds, thereby promoting mine roof monitoring. Another vital advantage is that a total station is more accurate than other roof monitoring since it does not attract both recording and writing faults (Gopi, Sathikumar, and Madhu 2008).

Regarding disadvantages, the manual operation takes a lot of time and human resources. A total station works well on the outside, and not from inside of the mine tunnels because indoor positioning is usually a challenge.

As such, monitoring the stability or weakness of a roof becomes a challenge to miners. A total station cannot be used at night, meaning that roof failure can go unnoticed up to the point of causing huge damages (Berg, Mitchell, and Proft 2008).

1.5.2.5 Cost. The cost of a total station in a mine is high compared to the other surveying instruments, thereby hindering its usage in mine monitoring. The costs of acquisition and maintenance are very high, thereby costing miners a large amount of cash in the purchase, installation, and maintenance. Precisely, the cost of standard total station costs is around \$ 5,000. Miners ought to be ready to incur these costs if at all they have to use total stations for monitoring their roofs.

1.5.3 LIDAR. This technique is broken down into 5 points.

1.5.3.1 Concept. Terrestrial LIDAR (Figure 1.9) can be termed as a ground-based laser scanner which is capable of producing high-quality 3D images of a mine's roof. The static acquisition terrestrial LIDAR is usually mounted on a tripod or even a different stationary device. As such, the static terrestrial components are vital in mines compared to its counterpart the mobile acquisition terrestrial LIDAR which is mounted on a vehicle. Important for underground work is the fact that its lasers are eye-safe.



Figure 1.9: The Leica® scan station LIDAR. LIDAR is one of the most modern laser-based scanners (Leica Geosystems AG 2017).

® Registered trademark of Leica Geosystems.

Terrestrial LIDAR gathers information that is very accurate and generates a dense point cloud, thereby enhancing the identification of objects. The laser capabilities enhance digital scanning functions which enable the miners to calculate changes in the structure of mine roofs easily.

1.5.3.2 Components. A LIDAR scanner is characterized by a laser source and detector, computer, LIDAR system, and a tripod. The laser generator creates the energy required for image capturing the roof's images. This detector detects the light pulses which reflect from the target.

The computer collects the (X, Y, Z) coordinate triplet information concerning a coordinate system where (0,0,0) scanner's location. Lastly, the computer is used to ascertain that all the other components work efficiently by integrating information from the laser system (Eitel, Vierling, and Magney 2013).

1.5.3.3 Installation. The installation process of LIDAR in underground tunnels requires miners first to assemble all the equipment needed. The next action plan entails installing LIDAR system on the tripod, establishing a connection with the computer, and fixing the laser equipment. The terrestrial LIDAR thus gains the ability to observe the well-being of an underground mine's roof.

1.5.3.4 Advantages vs. disadvantages. LIDAR enhances mine roof monitoring since it can collect information on millions of positions on an hourly basis compared to the other conventional systems. The equipment is simple to assemble, and the device can be used during the day and at night (Eitel, Vierling, and Magney 2013).

LIDAR is disadvantageous because roof monitoring can be a challenge when the source of power fails. Monitoring a mine becomes a challenge the utmost coordination is needed between the object used to generate and analyze the images. In this case, the device attracts a few challenges which ought to be addressed (Eitel, Vierling, and Magney 2013).

1.5.3.5 Cost. Using LIDAR in roof monitoring attracts a reasonable cost considering its suitable size and the affordability of the equipment. A single unit of a terrestrial LIDAR is sold from \$ 40,000 upwards, an aspect which limits many potential users (Eitel, Vierling, and Magney 2013). This equipment is highly costly, thereby hindering many people from using it in mine roof monitoring. Also, the results take

longer to release due to the lengthy process which can result in mine collapses if defects are not reported in time.

1.5.4 Extensometer. This technique is broken down into 5 points.

1.5.4.1 Concept. An extensometer is a device that can aid the measuring of changes in an object's length. There are three main types of extensometers, of which only one type is suitable for roof monitoring in underground mines.

The contact extensometer is excellent in mining since it is capable of conducting stress-strain measurements of a mine's roof by capturing images during the testing process. These device measures horizontal strains, as well as the settlements in rockfill or earth, fill dams and mines.

The subject tasks entail monitoring the settlement of foundations, excavations, and embankments (Ogundare 2015). The flanges of the extensometer work together with sensors which monitor mine roofs to detect any possibility of collapsing.

1.5.4.2 Components. The components of an extensometer include; a metallic rod and bolts (Heuvel 2003). Stability is key in the operations of an extensometer, an aspect which explains why metallic poles are used.

The extensometer is thus mounted on the pole using drilled holes which hold it firmly. All these components work together in monitoring the possibility of rock deformation, an aspect which causes mine roofs to collapse.

1.5.4.3 Installation. The installation of an extensometer in an underground mine environment begins by stabilizing the mounting pole which is in most cases fitted on the ground, outside the mine.

With the pole in place, the extensometer is attached and secured till it gets firmly attached. The other parts get fixed, after which the power source and laser source are all fixed. When the process is completed, the device is tested to ensure that it can easily monitor the changes in rocks deformation (Heuvel 2003).

1.5.4.4 Advantages and disadvantages. One advantage of an extensometer is that it is easy to use, thereby promoting the monitoring the behavior of displacement in the mine roof. Also, the device is easily portable, thereby enhancing its usability in various locations within the underground tunnels of a mine. The other advantage is that

the extensometer is powerful enough to provide real-time and accurate roof status information to the operator (Ogundare 2015).

The extensometer cannot cover a large area, the only thing it can do is to monitor a predetermined crack or fracture within the very small area. The evident disadvantage about extensometer is the high possibility of failure if the vibrations of mine roof and deformations are minimal. If kept in a noisy place, roof monitoring becomes a challenge, thereby increasing the possibility of its failure (Ogundare 2015).

1.5.4.5 Cost. The cost of an extensometer is appropriate for use since it is readily affordable and its usage is simple. This aspect makes it a suitable instrument for surveying since it enhances roof monitoring to the point of evading roof failure accidents (Heuvel 2003).

Mining companies have been using this device for a long-time due to its efficiency and affordability. Maintenance costs are also manageable, thereby making it a perfect tool for roof monitoring.

1.5.5 Photogrammetry. This technique is broken down into 5 points.

1.5.5.1 Concept. Photogrammetry refers to the scientific technique of making measurements by relying on photographs. This process is carried out by examining pictures portraying the exact surface point positions.

As such, photogrammetry can be easily applied to stereo pairs, or it can utilize remote sensing and high-speed photography. These techniques are usually used to record 2D and 3D motion areas by feeding imagery analysis and measurements to computational models.

In mining, terrestrial photogrammetry is applicable in roof monitoring operations (Milsom and Eriksen 2011). In mining, photogrammetry is utilized in calculating the measurements of the roof's stability or movements, and the information indicates all the observations. The camera is usually operated from a static point where it captures information regarding a mine roof.

Precisely, this equipment happens to be the simplest measuring instrument which gives out clear information with ease. The static aspect makes it easy for the camera to observe one region for a lengthy period of time, and numerous devices can be used to perform this task, hence enhancing mine monitoring.

1.5.5.2 Components. Photogrammetry relies on components such as a tripod and a camera. Image acquisition revolves around planning aspects such as making a good choice of the camera, taking photos, and its inspection. On the other hand, the control component entails the selection of the suitable location for ground inside the mine for purposes of collecting credible information as such; the control component is of great significance since it influences the capturing of high-quality images. The product compilation component is all about producing the end products, which are the images used in calculating the required measurements (Sužiedelytė-Visockienė 2013). Engineers are thus capable of utilizing this concept to conduct the measurements needed to run mines appropriately. The efficiency of each component is highly required in the imaging process to ensure that reliable results get accesses.

1.5.5.3 Installation. The installation process of photogrammetry, majors on bringing together of all the components required for the images to be captured. Computers, as well as the equipment needed to process film, are also set ready within the tunnels or from a monitoring station.

In a situation where the device cannot be mounted on a tripod, engineers can easily hold it since it is light in weight, an aspect which makes it portable (Milsom and Eriksen 2011).

Once processing is completed, the suitable computers are used in calculating the required measurements. The combination of all these aspects makes photogrammetry effective and a simple method of carrying out surveys.

1.5.5.4 Advantages and disadvantages. Terrestrial photogrammetry enhances mine roof monitoring by providing extensive information from the captured images. On a mining perspective, this concept creates a broad view of a target area because it identifies details regarding rock formation and the possibility of collapsing mines (Kraus 2007).

The other advantage is that the simple equipment and light weight aspects make it effective in capturing images from different sides of an underground mine. The low photogrammetry accuracy is the biggest disadvantage that makes it not useful in the field of roof fall monitoring.

The manual operation of photogrammetry equipment is quite tedious. Monitoring becomes a challenge if the device is handheld, and the person involved cannot be static. In this case, it is indisputable that with all these challenges, photogrammetry is highly unlikely to promote roof security (Kraus 2007).

1.5.5.5 Cost. Photogrammetry stands out as a very cost-effective survey method considering the ease of use and the accuracy associated with it. This aspect has succeeded in making photogrammetry an affordable practice which surveyors and engineers can rely on for proper planning of their mining activities (Kraus 2007).

As more developments continue to take place, the field of photogrammetry will end up advancing and solving numerous surveying problems.

1.5.6 Seismic Monitoring System. This technique is broken down into 5 points.

1.5.6.1 Concept. Routine seismic monitoring with the aid of seismic monitoring system in mines gives miners the ability to quantify seismicity exposure and offers a logistical tool. This guides the attempt of miners to prevent and control potential instabilities in mass rocks.

It helps to give alerts that precede the bursts of rocks. The objectives of using a seismic monitoring system to check rock mass seismic response are to rescue personnel, prevent, check hazard ratings, warnings as well as back analysis (Mendecki, Lynch, and Malovichko 2010).

Monitoring process and design of layout for mines are therefore enhanced with the aid of seismic monitoring system.

1.5.6.2 Components. Seismic monitoring systems usually have various components which enable them to detect ground movements. These components include a sensor, a recording system, and a transmitter, and a display unit.

The sensor plays the task of detecting ground movements since it is usually placed beneath the earth's surface. After detecting roof failure activities, the vibrations are transferred to the recorder using wires.

The recorder thus gets the chance to record the collected information for analysis and record keeping purposes (Olsen, Raugust, and Roe 2013). It is through this every data regarding the possibility of a failure is recorded, thereby enabling engineers to plan safe mining.

The satellite transmitter is essential considering the fact that real-time information gets passed to the involved seismology facilities.

1.5.6.3 Installation. Seismic monitoring systems have the simplest installation process among the roof monitoring instruments required in underground mining roof monitoring. The first step is to entail that one has all the components ready, as well as the other supportive equipment. The sensor is then dug beneath the ground where it can easily sense the up and down movements of the roof inside the mine (Kayal 2008). The other step is connecting it to the recorder which has to be well-positioned in a place where the recordings cannot be tampered with. The last step is the positioning of the satellite transmitter which after being connected to the recorder can easily send signals of the roof movements, and ensuring that the screen is on to portray all the data collected.

1.5.6.4 Advantages and disadvantages. One advantage of seismic monitoring equipment is the ability to keep credible records of the exact activities happening on the ground in an underground mine. The other advantage is that the setup is easy, and so is the interpretation of the recordings (Kayal 2008). The availability of cheaper seismic monitoring systems makes the job easy for seismologists, thereby enabling them to accomplish their professional goals and objectives (Olsen, Raugust, and Roe 2013). In most cases, mine workers perish in underground mines due to the lack of an early warning.

To be precise, these systems do not detect roof failure, but rather they record when they are taking place. This aspect explains why numerous lives have been lost around the world even in places where the devices had already been installed. Another challenge is that once an earthquake occurs, seismic monitors are not able to identify the direction it heads to. As such, the calamities associated with earthquakes end up affecting many people (Kraus 2007).

1.5.6.5 Cost. The cost of seismic monitoring systems is favorable in monitoring mine roofs. While the most sophisticated ones are costly, the simple ones tend to be quite cheap. A simple seismometer can be acquired at a price ranging between \$ 13,000 and \$ 20,000. On the other hand, the complex ones can cost as high as \$ 30,000 or even more. The same case applies to the running and maintenance operations since lots of money have to be spent to evade unnecessary faults (David Funkhouser 2011).

2 USING LIDAR FOR MEASURING THE PRECURSOR MOVEMENTS

2.1 CAPABILITIES OF TERRESTRIAL LIDAR

LIDAR stands for LIght Detection & Ranging which uses laser light to illuminate a small point on an object and then receive the reflection of that light to analyze its intensity, amplitude and the time of flight of the light from sending until receiving the back reflection. The light of most LIDAR scanners uses the visible spectrum or near visible spectrum. The visible spectrum occupies 390 nm - 700 nm. Terrestrial Scanning (Figure 2.1) creates 3D models of complex objects such as piping networks, roadways, archeological sites, construction sites, and bridges.



Figure 2.1: Terrestrial LIDAR (Murphy Surveys Ltd 2017).

The LIDAR scanner generates very fast pulses of the laser light projected on an object; the pulses might be around 150,000 pulses/second or more. An internal sensor on

the device measures how long it takes for each pulse to return again to the same source (in the case of a time-of-flight LIDAR scanner). The light is moving at a constant speed so the LIDAR instrument can calculate the distance between itself and the object. By repeating the process of sending pulses and receiving it back again in quick succession over different parts of the surface of the object, the instrument can generate a 3-D 'map' of the object it was scanning. With ground-based LIDAR a single GPS location coordinate can be attached to each object where the device is set up. From this technique, it is clear that the LIDAR device work principal depends on the active energy which capable of working in both day or night because of the light emitter presence.

This raw data set, called "point cloud," contains many points in the same dataset which can be many millions of points, and its accuracy can range from 1 cm to sub-millimeter in some cases. On a typical scanner with an integrated optical camera, every single point can be associated with four different parameter combinations:

- ❖ The (X, Y, Z) point location coordinates per single point.
- ❖ The (X, Y, Z) point location coordinates plus the intensity (I) of the light returned to the receiver component per single point.
- ❖ The (X, Y, Z) point location coordinates plus and the color information carried out to the receiver (R, G, B) per single point (Note that RGB information is collected by a camera synchronized to the LIDAR scan).
- ❖ The (X, Y, Z) point location coordinates, the intensity (I) of the light returned to the LIDAR, and the color information carried out to the receiver (R, G, B) per single point.

X, Y, Z refer to the cartesian coordinates of that particular point. The letter "I" relate to the intensity of the light pulse returned to the receiver, and depends on the strength of the laser, the distance between the target and the reflectivity of the target.

R, G, B, refers to the red, green, and blue colors information gathered by the optical sensor and assigned to the nearest LIDAR generated segment. Some of the LIDAR scanners have built-in optical sensors (cameras), on the other hand, some the scanners do not have that feature, so that type can not provide the (R, G, B) color data information.

The point cloud data set can be viewed after scanning for some scanners in real-time as the image is being produced. The conventional techniques like the tapes, theodolites or even the more updated technologies such as the total stations and GPS can not provide the same accuracy in the same time frame (Addison 2000).

3D laser scanning technologies can be used to detect and record a significant number of objects in different size scales such as structures, topographies, or bridges. Today, LIDAR technology is developing fast.

The processing stage of the point cloud data set can be done thru many software applications to export to a large variety of applications such as CAD programs, contour maps, 3D models. Three-dimensional scanning technologies are based on one of two methods. There are two principal types of laser scanners depending on its method of measuring (San Jose Alonso et al. 2011).

The first one is the time-of-flight, and the second one is phase-shift, both of which collect similar data and below is a brief comparison between the two methods, (Frei, Kung, and Bukowski 2005) as follows:

- ❖ Time of Flight: In the direct time-of-flight measurement method, a rhythmic pulse is emitted, and one or even many timers measure the time difference starting from the time of emitted pulse and ending with the reflected pulse arrival time. This time resultant can quickly provide the distance, according to the following equation:

$$\text{Distance} = (\text{Speed of the Light} * \text{Time}) / 2 \quad (2.1)$$

The speed of light is constant, and it is equal to 299,792,458 m/s in a vacuum. The division by two is because light travels from the sensor to the object and returns to the sensor.

- ❖ Phase shift: The major difference is that the distance can be measured thru this method comparing the difference in the phase of the emitted light vs. the reflected light.

The instrument emits a stream of pulses which have a predetermined frequency and phase then by comparing the outgoing phases to the incoming

phases to get the difference as a result of the phase shift method. After that the time-of-flight is calculated using the following equation:

$$\text{TOF} = (\text{Phase Shift}) / (2\pi \times \text{Modulation Frequency}) \quad (2.2)$$

Terrestrial LIDAR can also be useful to provide data to Digital Terrain Models (DTM's) with a georeferenced point cloud data set or be used to create a Triangulated Irregular Network (TIN). The LIDAR scanner allows the quick and accurate dense 3D point cloud data was collected as in (Figure 2.2).

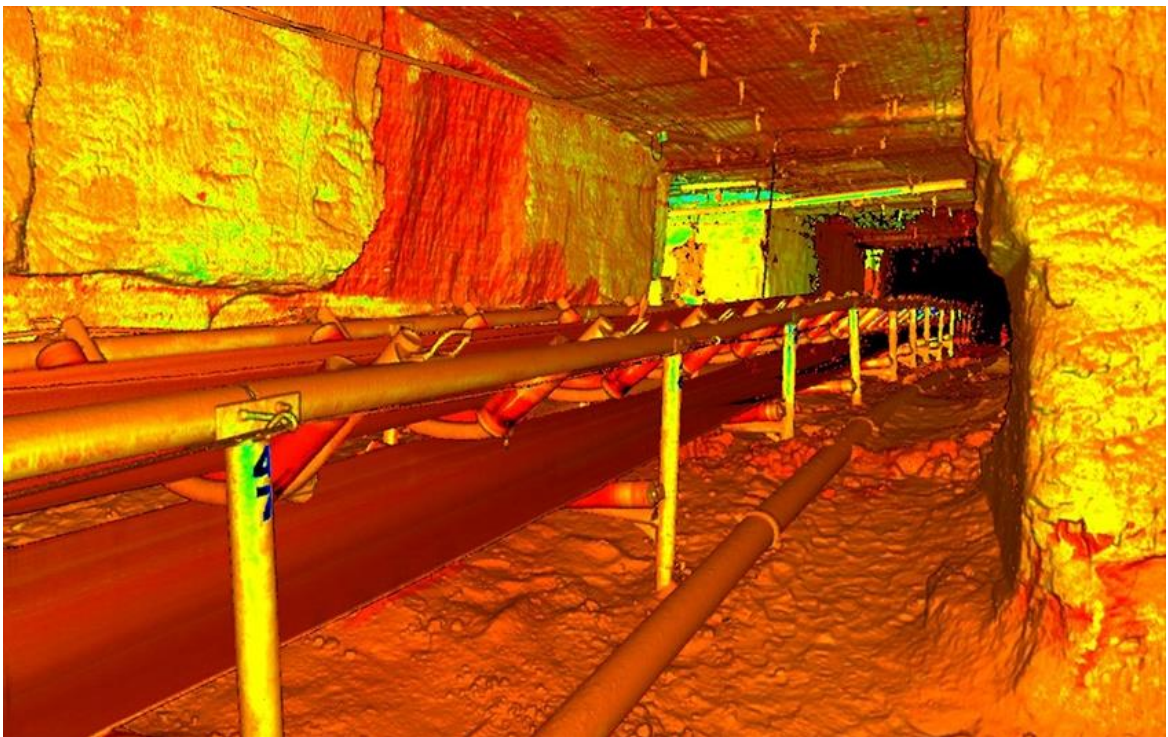


Figure 2.2: Dense 3D point cloud data collected by terrestrial LIDAR (African Consulting Surveyors 2015).

2.2 USE OF INEXPENSIVELY FIXED LIDAR SCANNERS

The terrestrial LIDAR has been described in the previous section, and it is very important to mention that for many real projects, considering using a terrestrial LIDAR is too expensive. It is a relatively large and heavy machine that consumes significant power (Sheh et al. 2006). The previous paragraph shows that the terrestrial LIDAR has major disadvantages that might be a real motivation to use inexpensive fixed LIDAR.

This current research will explore the feasibility of the inexpensive fixed LIDAR in roof failure detection. The positive effect of this inexpensive LIDAR technology is that every part of this signal processing can be performed in a single microchip. That means pulsed light devices do not need to use extra hardware components to perform signal processing like clocks used in many time-of-flight systems. The inexpensive LIDAR scanner is not good enough for construction or surveying applications, however the advantages of the inexpensive include:

- ❖ Low cost (\$100-\$1400).
- ❖ Low power (less than 5W).
- ❖ Lightweight (less than 250g).
- ❖ Small size.
- ❖ Wide Beam View.
- ❖ Robust (capable of the move and mounted in any situation).
- ❖ Simple one port computer interfacing.

The ultrasonic sensors fall within the same cost range of the inexpensive LIDAR. However, the ultrasonic sensors only have an accuracy range about 1 to 250 cm while the inexpensive fixed LIDAR accuracy range is about 50 meters.

The ultrasonic sensors are also very sensitive to the change of the temperature, pressure, and other environmental effects. Additionally, the accuracy of the ultrasonic sensor is inversely proportional to the detected distance. Two alternative technologies for distance measurement are infrared proximity sensors, and the other one is the LIDAR. The detected data shows that the infrared technology has a shorter range of 5 to 80 cm resulting in the same limitations with the ultrasonic sensors. The infrared technology accuracy decreases in as distance increases (Duong et al. 2012).

Lasers, on the other hand, can measure further distances with a higher accuracy. Lasers were relatively expensive when compared to ultrasonic sensors and infrared sensors, but not anymore.

In these days it is possible to purchase inexpensive LIDAR devices costing no more than \$2,000 to make distance measurements more accurately than most any other technology with a detection range of up to 50 meters (Duong et al. 2012).

The ultrasonic range is very short, approximately 5 meters and with the traditional beam width around 9° compared by the laser sensors which has higher beam width, approximately 45° and high detection range up to 50 meters.

Some ultrasonic sensors have a very narrow beam, approximately 25.4 mm. A laser distance sensor wins on every aspect: speed, accuracy, safety, reliability, and functionality. Ultrasound sensors provide various of the similar features but are less accurate.

Traditional LIDAR sensors are used in spacecraft, autonomous cars, surveying machines, robots, and law enforcement tools. These applications are high-end and not applicable to the scope of everyday life, as it needs a high measurement frequency and expensive technologies.

Recently, however, low-cost tools that implement LIDAR have entered the market, allowing hobbyists, not just large organizations, to develop this technology. In another hand, there are some other inexpensive technologies such as ultrasonic sensors, but these have some limitations.

Inexpensive LIDAR sensors have been produced widely in the late ten years, which easily measure the distance to nearby targets without any physical contact. For example, the (leddar[®] M16 sensor) can be utilized for object detection in the field of view (FOV) of the sensor.

The optical design defines the FOV of the sensor. Leddartech provides various configurations, in addition to the optics that can be tailored to a specific application to match the FOV to the required detection zone. Inexpensive LIDAR can be utilized in the automotive application.

[®] Registered Trademark of Leddartech Incorporation.

In fact, the LIDAR technology is the only validated technology for object detection. For example in vehicles technologies, the LIDAR can detect 99/100 objects if installed on a car which indicates high ability in object detection (Louay Eldada 2014).

Inexpensive LIDAR sensors can be used in smart homes such as the smart home lighting. Smart home lighting can be designed with computer software connected to the inexpensive LIDAR; this mentioned system is capable of detecting the ambient moving objects in predetermined range using the LIDAR sensor. The activities which are detected by the inexpensive LIDAR can be utilized as a trigger for any action that the engineer would like to do such as: turning the light on or off or any other selective appliance in home automatically when there are no activities around the sensor.

One of the most significant benefits of the mentioned system is decreasing the energy and power consuming; therefore the costs will be less. The most important fields that inexpensive LIDAR sensors involved in successfully are:

- ❖ Home and it Mapping.
- ❖ Tracking & Speed Measurement.
- ❖ Automotive , Collision Avoidance & Navigation.
- ❖ Smart Lighting.
- ❖ Drones And Mapping.
- ❖ Industry Machine Safety.
- ❖ Security and Surveillance.

3 PURPOSE OF THIS RESEARCH

The purpose of this thesis is to evaluate a single LIDAR sensor which is the M16 scanner designed by Leddartech company for the purpose of integrating into an Early Warning System (EWS). The early warning systems can be defined as “monitoring devices designed to avoid, or at least to minimize, the impact imposed by a threat to humans, damage to property, the environment, or/and to more basic elements like livelihoods”(Medina-Cetina and Nadim 2008). In fact, the main goal of this thesis is to prove and validate the feasibility of using low cost small solid-state LIDAR sensors to detect ground movement. The goals of this project are:

- ❖ To develop a monitoring tool capable of detecting rock movement at a resolution that is sub-millimeter. The sensor must have high accuracy, precision, and repeatability.
- ❖ Provide a reliable monitoring tool at an affordable cost. The sensor must be relatively inexpensive and have a high data rate.
- ❖ Provide an integrated system that can monitor the roof fall remotely without any need to install or attach any instrument to the projected roof. The sensor must measure small displacements using non-contact methods.
- ❖ Finally, it is important that the tool provides an open environment allowing the developers to enhance the tool and track the procedures of the movement detection by logging out the detected data in the .txt file format or even excel sheet. The user interface which allowed the user to export the data in the preferred format can be a perfect solution that it will be added to this project.

The sensor must have a digital interface to allow automated data acquisition.

Upcoming research will be concentrated on building the EWS's in an underground mine, and that should be of course after finishing the validation of the inexpensive LIDAR in underground movement detection.

4 RESEARCH TOOLS

4.1 DEVELOPMENT OF A ROCK DISPLACEMENT SIMULATOR (RDS)

The roof failure is one of the main problems which the inexpensive LIDAR will monitor to verify whether it is reliable to detect the roof failure.

4.1.1 Introduction to the Rock Displacement Simulator (RDS). The roof failure and the detector are the main components of this project. The roof failure is the problem that the inexpensive LIDAR will be monitoring to verify whether it is reliable for detecting the roof failure or not.

An inexpensive LIDAR has been selected, but it was a quiet difficult to monitor a real mine roof due to the inability to predict the moment of the roof deformation. So one idea has been raised can be summarized in the following two points:

First: Roof failure can be simulated by a target plate of any solid material, moved by a linear actuator. The most important at this point is to find an actuator that can provide the accurate stepping mechanism to simulated the small movements found in unstable mines roofs.

Different types of the linear actuator work in a variety of ways and every one of the actuators can be beneficial in specific a applications, the different type of actuators are as follow:

- ❖ Mechanical actuators:
- ❖ Hydraulic actuators:
- ❖ Pneumatic actuators:
- ❖ Piezoelectric actuators:
- ❖ Electromechanical actuators:

Many mechanisms are employed to generate straight line motion from a rotating actuator motor as follow:

- ❖ Screw
- ❖ Wheel and axle
- ❖ Cam

The actuator that has been used in this thesis is a screw actuator working on the principle of the threaded rod which is moving linearly due to rotating of the actuator's nut (Sclater and Chironis 2001).

The main idea that the rock displacement simulator (RDS) is to simulate the rock movement precisely. The best solution has been found the EZ-Limo[®] NO. (EZC4-05M) which is electromechanical linear actuator designed by Oriental motor USA corporation which generates the linear motion based on the screw mechanism.

A linear actuator is an actuator that makes a straight line motion. Linear actuators are used in industrial machinery such as printers. Hydraulic, pneumatic and piezoelectric actuators inherently provide straight line motion. (Controls International LLC Fisher and Emerson Process Management 2005).

4.1.2 Concept. The roof failure inside mines moves in typical stages of creep movement which was explained previously. The typical curve starts with the primary stage and ends up with the tertiary stage which is the stage before catastrophic failure.

The rock failure can be simulated as mentioned before in section 4.1.1 using a linear actuator. The concept behind the rock displacement simulator is to design a platform that can move precisely. The platform will be moving like a rock block inside the mine. The movement of the platform should be smooth and slow to act as the rock would move before the moment of catastrophic failure. The system of the (RDS) components is explained in the next point.

4.1.3 Components. The components of (RDS) is broken down into 4 points.

4.1.3.1 Target plate. A rock movement simulator or motion platform is a mechanism that creates the small linear movement of a target plate that simulates rock movement acting as precursors to roof falls, pillar failures, and rock bursts. It is designed to simulate the movement of the roof deformation. When motion is applied and synchronized to horizontal or vertical movement, the result is a combination of sight movement/acceleration. A sturdy and heavy frame has been built to make the electromechanical linear actuator stable while moving the target plate to a certain profile

[®] EZ-Limo Easy Linear Motion is a registered trademark of Oriental Motor Corporation, LTD in Tokyo and other countries.

(Figures 4.1 – 4.3). The dimensions of the target plate (Figure 4.4) are in the rectangular shape with a width of 457 mm and length 610 mm. The most important thing in the platform is to be enough surface area to include at least four M16 scanner segments. The M16 will detect the mentioned four segments in every test. These four segments will determine the distance between the target plate and the M16 scanner while the target plate is moving.



Figure 4.1: The process of constructing the actuator frame. Eliminating the sharp edges of the actuator frame to make it hand safe.



Figure 4.2: The welding process of the actuator frame.

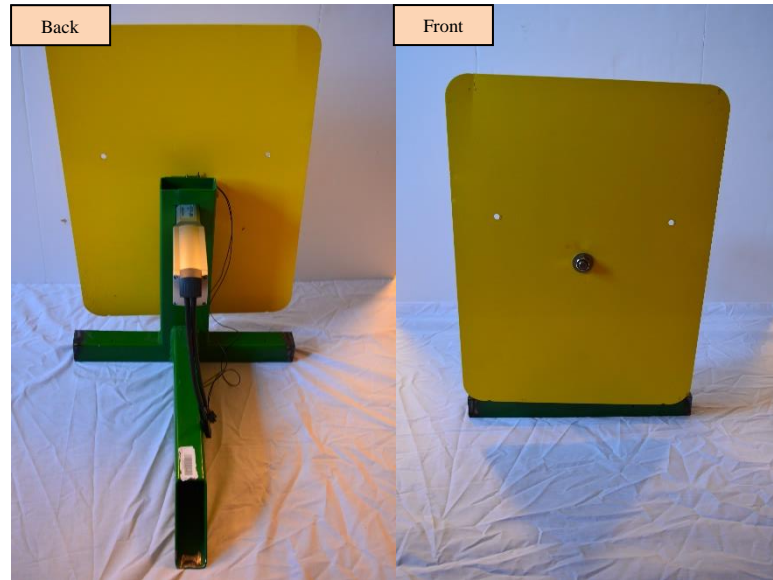


Figure 4.3: The final design of the actuator. Yellow target plate, and its green frame.

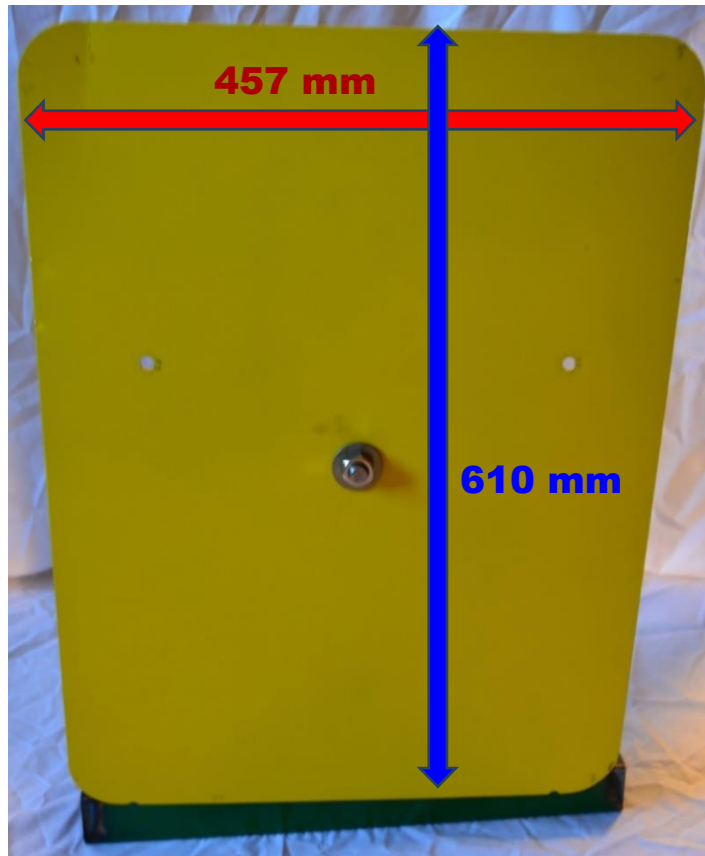


Figure 4.4: Front view of the target plate.

4.1.3.2 Linear actuator EZC4-05M (specifications). The linear motion actuator mechanism chosen for this thesis works on the principle of the screw mechanism. The screw mechanism can generate very precise motion which helps to simulate the slow movement of rock. The precise movement of the screw mechanism actuator relates to the ball screw inside the actuator which is rotated by a motor to a specified position. Even with heavy objects, it can be moved precisely. This actuator is essentially compatible for applications where the load is pushed or pulled. In the mechanical screw mechanisms, the screw shaft can rotate inside a threaded hole in a stationary module, or a threaded nut can rotate around a stationary screw shaft (John Cave 1995). The EZ Limo EZC4-05M electromechanical linear actuator (Figure 4.5) utilized in this project move linearly back and forth to reach the desired position, and the standard curve of rock deformation can be simulated. It is compact actuator specially designed to fit the motor and the actuator components into the smallest possible size (Oriental Motor 2004).

It incorporates a lead screw and lead nut while using a ball screw and ball nut. EZ limo motorized cylinder actuator is a linear-motion system that combines oriental motor's pledge, utilization of the latest motor technology, the pursuit of mechanical design excellence (Oriental Motor 2004). Originally the linear actuator has been used in this thesis provides a linear movement with an accuracy up to 0.06 mm per step and ± 0.02 mm repetitive positioning accuracy (mm).

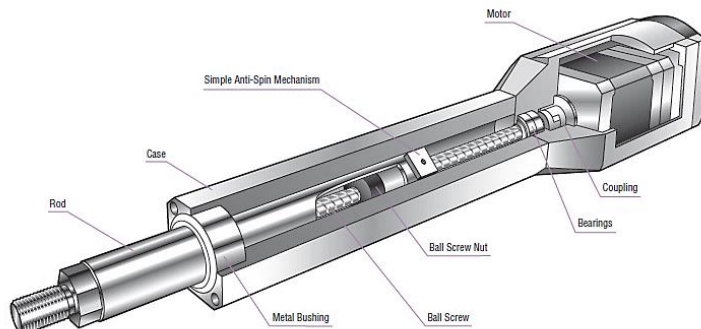


Figure 4.5: The EZ Limo EZC4-05M electromechanical linear actuator (Oriental Motor 2004).

4.1.3.3 Control circuit. The control circuit parts are broken down into 7 points.

4.1.3.3.1 Introduction to the control circuit. Stepper motor drivers translate pulse signals to the motor from the controller to attain an accurate positioning. It is the chips that retain the power that drives the motors to be detached from the power on the Arduino (Morar 2011).

Since the Arduino® microcontroller is not able to provide sufficient current needed to power the stepper motors, the user directly, therefore, has to utilize separate chips to function as switches that manage the spinning of the motor.

The stepper driver chips are also beneficial in providing fractional steps. This aids in smoothening out the stepper motor movement (Morar 2011). Stepper motors can attain elevated rotation speeds by the use of microcontroller based steppers drivers.

While using a microcontroller, it is plausible to attain control on how each individual coil is stimulated while in the motor. It is essential in obtaining high speed since as the speed increases the point in time of the firing of the coils ought to be absolutely in sync (Bogdan 2011).

The stepper motor in this thesis provides 16X micro-stepping which is 16 times the precision of the original actuator. The (Figure 4.6) shows the microcontroller- based precision rock displacement simulator (RDS) circuit.

The assembled board has the major components (Arduino® microcontroller, stepper driver, power electricity supply, and radio transmitter). It is constructed having the ability to accurately displace a solid surface in increments of 0.015 mm, operated under radio control.

The control circuit originally consists of a microcontroller board wired to a ZigBee® radio and other support circuitry. This rock displacement simulator (RDS) device can be operated under remote radio control and will be used to evaluate all displacement sensors in the office environment.

® Registered trademark of ARDUINO AG, LLC.

® Registered trademark of Digi International Incorporation.

The rock displacement simulator can be programmed to move in several different motion profiles for both static and dynamic sensor evaluation tests and to simulate the type of slow, long-term displacements typically occurring in unstable mine walls and roofs.

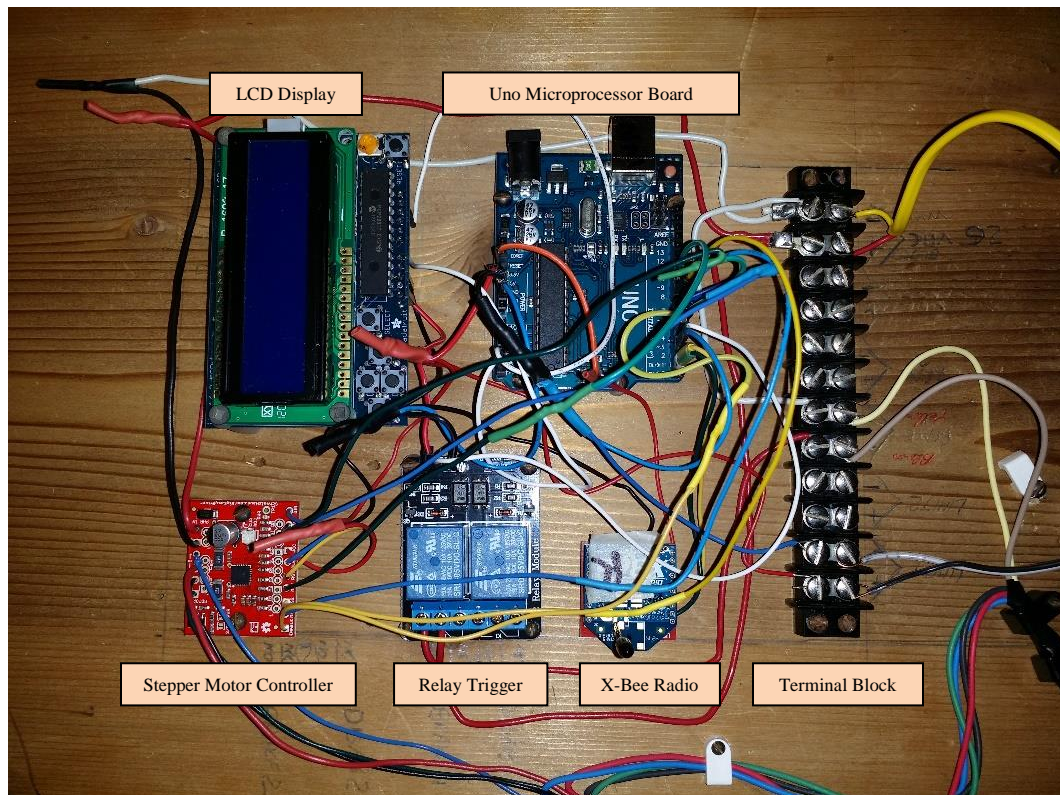


Figure 4.6: Prototype of the programmable actuator circuit.

4.1.3.3.2 Stepper motor drivers. Stepper motor drivers translate pulse signals to the motor from the controller to attain an accurate positioning. It is the chips that retain the power that drives the motors to be detached from the power on the Arduino (Morar 2011). Since the Arduino microcontroller is not able to provide sufficient current needed to power the stepper motors, the user directly, therefore, has to utilize separate chips to function as switches that manage the spinning of the motor.

The stepper driver chips are also beneficial in providing fractional steps. This aids in smoothening out the stepper motor movement (Morar 2011). Stepper motors can attain elevated rotation speeds by the use of microcontroller based steppers drivers. While using a microcontroller, it is plausible to attain control on how each individual coil is stimulated while in the motor.

It is essential in obtaining high speed since as the speed increases the point in time of the firing of the coils ought to be absolutely in sync (Bogdan 2011). The stepper motor in this thesis provides 16X micro stepping which is 16 times the precision of the original actuator.

4.1.3.3.3 Trigger relay module. The trigger relay module is an electrically operated switch which is used to isolate two circuits electrically. This switch powers on and off the current by using electrical signals. A variety of sizes, shapes can be found in the relay on modules, and multiple types of singular contacts are available for different applications.

The trigger relay module is used to provide at all times protection for the actuator. Relay module facilitates its users by offering many kinds of functions. It can easily control larger electrical devices and loads, for example, AC or DC motors, electromagnets, etc.

Different packages of single or multiple contacts are available with relay modules where bigger power relays operate the primary current (Sidhu, Ghotra, and Sachdev 2002). In short, we can say that relay module is an automatic stable and long term reliable switch that can control high current circuit through its small current signals. The trigger relay module is extensively used in devices used for power protection, remote controls and automation technology appliances (Park, Sthapit, and Pyun 2009).

4.1.3.3.4 X-bees radio (transceiver). X-bees can be described as an advanced radio frequency trans-receivers, which are capable of sending and receiving data through serial ports, which can be extended into diverse multi-unit meshed X-bee networks either as a pair exchanging data or X-bees can be utilized in divergent ways. For instance, X-bee could be used to operate a robotic machine to investigate the environmental conditions. X-bee radios have been discovered with myriads of different features. X-bees

modules are illustrated as an embedded solution to provide wiring end point connectivity for multiple devices.

X-bee especially uses a kind of a protocol to enable data communications with additional features that are considered to be prominent for robust network communication. Quality features have eased the work burden of users. Certain features vary from addressing the acknowledgment and some retries that are beneficial or useful to impart secured data across users.

4.1.3.3.5 Arduino UNO microcontroller (MCU). The UNO microcontroller is simply used for interfacing software and hardware. The UNO is considered to be a paramount board that one can utilize when starting coding and electronics. For the beginners, it is critical for them to understand that UNO is believed to be the most powerful board that new users can get, to begin with. UNO is the most recognized and utilized board in the entire Arduino and genuine lineage (Barrett 2013).

It comes outfitted with a fourteen digital input and output pins, six analog inputs, an extra quartz crystal of 16 MHZ, a power jack, USB connection, a reset knob and an ICSP header (Boxall 2013). It comes fully packaged with tutorial booklet plus some cables required to support the microcontroller when connecting it to the computer by the use of USB port. Another option is by powering it up by use of a battery or the AC-to-DC adapter to start it (Boxall 2013).

4.1.3.3.6 Liquid crystal display (LCD). A liquid crystal display can reproduce an image based on optical phenomena of electrically controlled birefringence and polarization. Using microcontroller makes the system simple, efficient and flexible to display content on LCD. Since the microcontroller was controlled by software, the hardware complexity reduces tremendously. If modification of operation is needed it can be done very easily (Md. Khalid Hossain et al. 2015).

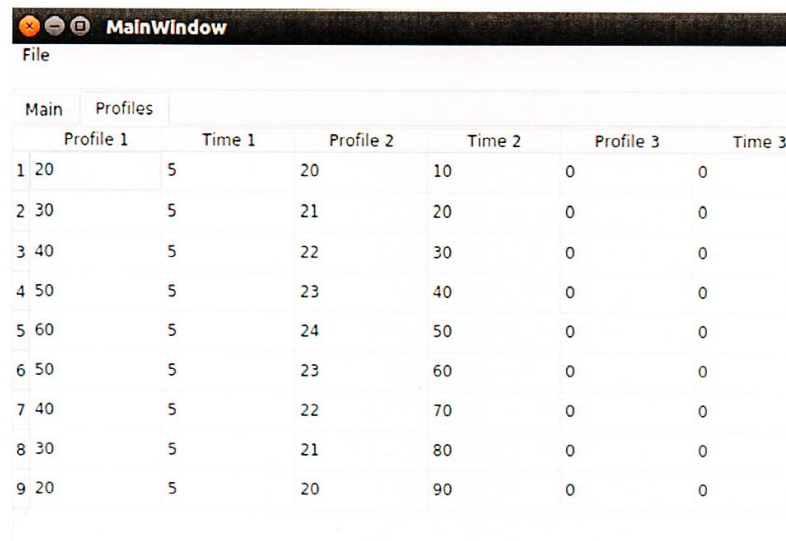
Light-emitting diodes (LEDs) have been used in liquid crystal display (LCD) devices, some of the LCD devices are calculators, televisions, mobiles, etc. LCDs with LED backlight units helps to achieve good quality display, for example, 16x2 LCD can display 2 lines, each line has 16 characters, and each character displays 15x7 matrix. The optical quality of all LCD devices is based on light source (Chen 2011).

4.1.3.3.7 Volts of direct current (VDC) power source. Two batteries and one cable power supply needed electricity to run the actuator. Two 12 volt batteries are used to power the system. The power in one battery is considered fully charged is 12.6 volts or higher, so the total voltage is about 25.2 volts.

The two batteries are responsible for providing enough power to move the actuator to the designed profile which will be simulating the rock movement.

4.1.3.4 Software control. A GUI (Graphical User Interface) was built for the rock displacement simulator using QT for the GUI builder and Python® for the event handling (Figure 4.7). Any number of displacement profiles can be defined, each having any number of definition points. The profile definition can be programmed with be variable- time- intervals. The variable- time- interval provides the capability for defining realistic displacement profiles and allows for longer profile durations. Profiles may be ingested using CSV (Comma Separated Values) files.

All processing parameter is accessible via the GUI (Graphical User Interface). This design facilitates power off operation of the simulator microcontroller since most of the control logic was removed to a remote controller.



The screenshot shows a window titled 'MainWindow' with a 'File' menu. Below the menu is a table with columns for 'Main', 'Profiles', 'Profile 1', 'Time 1', 'Profile 2', 'Time 2', 'Profile 3', and 'Time 3'. The table contains 9 rows of data.

	Profile 1	Time 1	Profile 2	Time 2	Profile 3	Time 3
1	20	5	20	10	0	0
2	30	5	21	20	0	0
3	40	5	22	30	0	0
4	50	5	23	40	0	0
5	60	5	24	50	0	0
6	50	5	23	60	0	0
7	40	5	22	70	0	0
8	30	5	21	80	0	0
9	20	5	20	90	0	0

Figure 4.7: Screenshot of the simulator program.

® Python" is a registered trademark of the Python Software Foundation ("PSF").

The sensor must be relatively inexpensive and have a high data rate, so the software has been built in a GUI interface for the rock movement simulator using QT for the GUI builder and Python® for the event handling.

In the (Figure 4.7) the numbers 20,30,40,50,60, in the column titled “Profile 1” from top to bottom refer to the displacement in mils that the software will request the actuator per time to move.

The “Time 1” column refers to the time period needed per row movement. For Example, the row NO. 1 shows that the software will send a request to the actuator to travel from the original state until 20 mils (0.02 inches) = 0.508 mm and this travel should be done in 5 seconds.

The rock displacement simulator (RDS) computer sends commands to the actuator to move to a predetermined profile (Figure 4.8).

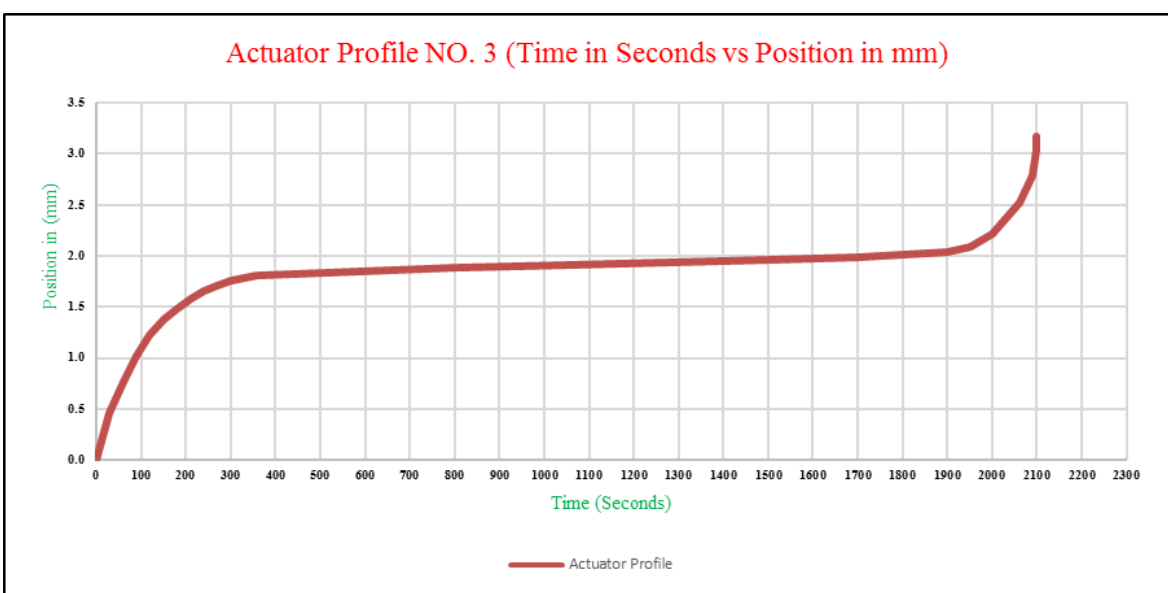


Figure 4.8: One profile that has been used in the simulator program.

In the meantime, the scanning process using the M16 scanner starts recording the data to another computer named (RDD) rock displacement detector.

4.2 THE LINEAR ACTUATOR MODIFIED PRECISION CALCULATIONS

The internal stepper motor inside the actuator has 200 full steps per revolution. The stepper motor driver chip mentioned in the section of the control circuit components provides a 16X micro stepping, so that moves the actuator a number of steps per one revolution equal to:

$$200 * 16 = 3200 \text{ steps per revolution} \quad (4.1)$$

The internal lead screw inside the EZ Limo EZC4-05M electromechanical linear actuator has a pitch of 12 mm - that means for every revolution, it moves 12 mm. So the modified resolution that the stepper motor driver can create as follow:

$$\text{mm per step} = 12 \text{ mm} / 3200 \text{ steps} = 0.00375 \text{ mm per step} \quad (4.2)$$

4.3 VERIFICATION

The target plate and the control software should work properly to generate the designed profile which will help to validate the M16 sensor. The proper behavior of the target plate/control circuit can be tested by varieties verification tools.

One method has been used to check that the target plate software simulator is working properly and sending the right and exact movement profile.

The verification step is very important before collecting the data. The verification needs to be accurate and repeatable.

The method that has been used is by attached dial gauge (Figure 4.9) to the front of the yellow target plate then start to run the simulator program to a certain distance.

If the specified distance by the simulator software was as measured by the dial gauge, then it is working properly.

Finally, a series of program moves compared to what it has been read on the dial gauge has been verified.

The first move driven by the software was from (0 mm – 0.254 mm). The second one was from (0.254 mm – 0.508 mm). All moves have been verified correctly with the dial gauge readings.

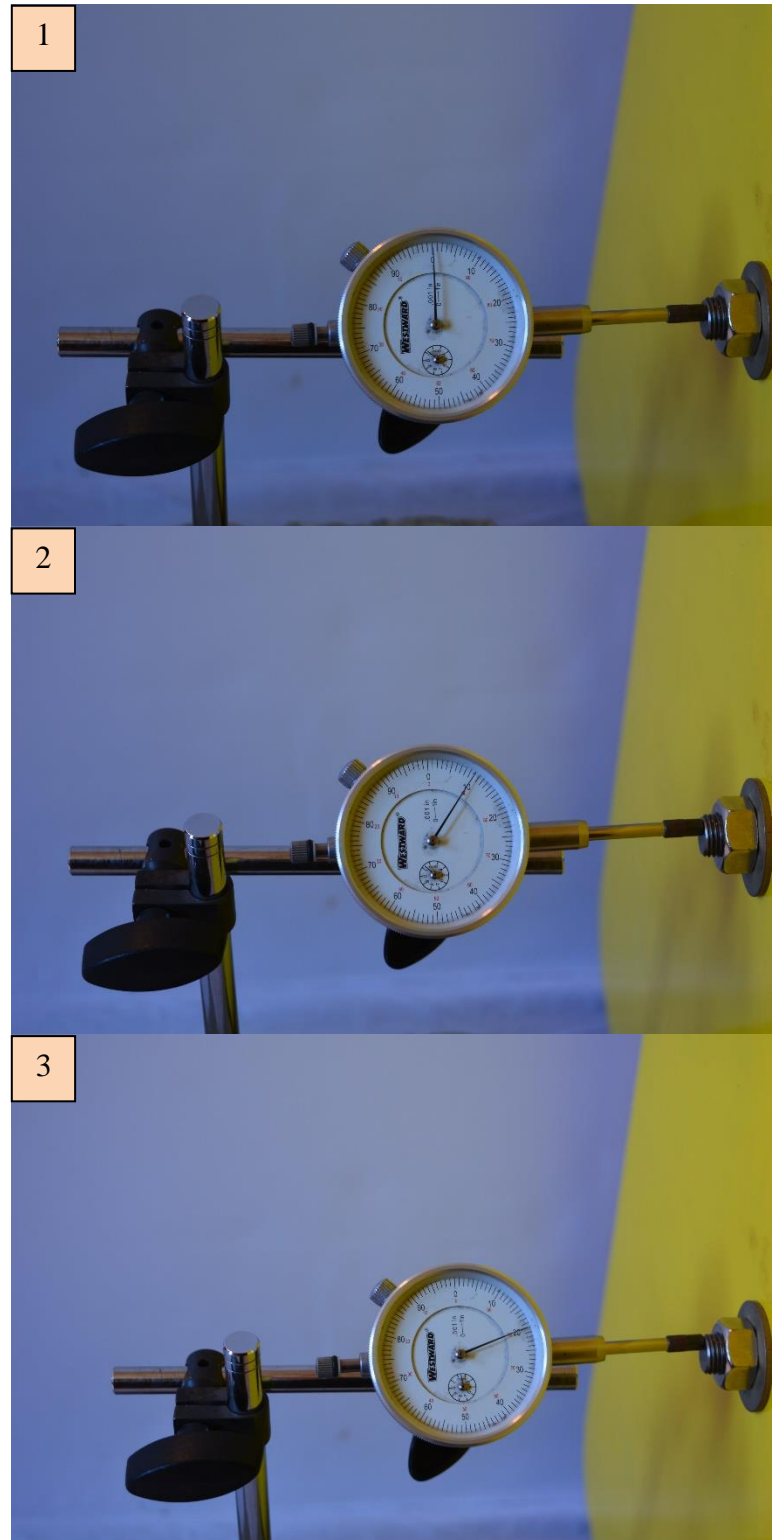


Figure 4.9: The yellow target plate is moving toward the dial gauge. The reason after installing the dial gauge is to monitor the real actuator movement. This procedure is to verify the rock displacement simulator accuracy.

4.4 USING THE M16 SCANNER

LIDAR technology has been used extensively in different applications worldwide. Solid-state LIDAR exposes up the potential of less one thousand dollars powerful LIDAR tools, which today can easily cost approximately \$100k/unit.

4.4.1 Introduction to the M16 Scanner. LeddarTech company is one of the leaders in this market. Solid state LIDAR, fixed detectors basically designed as a smallest size embeddable sensor which has the lowest possible cost. The fixed sensors are miniaturized to be embedded. From a cost standpoint, both contain lenses, lasers, and detectors. The lowest cost system is actually via surround view sensors because rotation reuses the lens, lasers, and detectors across the field of view, versus using additional sensors each containing individual lenses, lasers, and detectors. This reuse is both the most economical, as well as the most powerful, as it reduces the error associated with merging different points of view in real-time—something that really counts when the vehicle is moving at speed.

The main reasons that make the LIDAR technology reliable in the different applications are the accuracy that LIDAR can offer, in addition to the fact that LIDAR scanners are not impacted by the surrounding factors as much as the other different technologies, and the ease of utilizing the LIDAR technology.

On the other hand, the cost of the LIDAR is very expensive, and this might be the most important reason that prevents users from using this technology. The price of the normal LIDAR (terrestrial LIDAR) scanners range between \$35,000 to \$120,000.

So there is a need for another choice that can provide the similar accuracy at a significantly lower cost. Inexpensive solid state LIDAR scanners have become one solution to the problem of high cost of the terrestrial LIDAR.

4.4.2 M16 Scanner and Software Developers. The M16 (Figure 4.10) was developed in the summer of 2013. The M16 scanner is essentially made for traffic application such as on-road obstacle detection and tracking of vehicles. Moreover, the M16 scanner can be a great tool for many other monitoring implementations. The M16 has exposed at the AUVSI unmanned systems conference to promote the possibilities and potential use of the M16 in the unmanned vehicles research field. The

M16 uses two high-power light-emitting diodes (LED) as illumination source instead of a laser light source.

The sensor has sixteen channels built into a photodetector array which collects the energy of the emitted light that is reflected by the scanned objects (Bill Gutelius 2014).

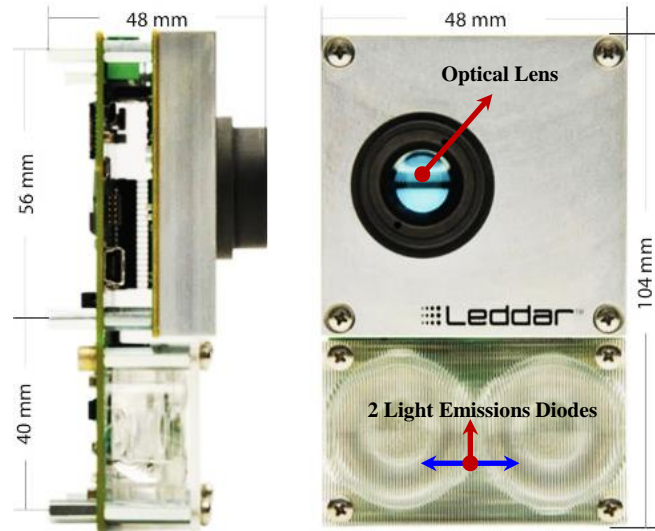


Figure 4.10: M16 scanner dimensions. The two light emitting diodes (emission optics) send the light pulses, and the lens (reception optics) records the light pulses reflected from the target (“Evaluation Kit and Configurator User Guide” 2015).

4.4.3 Properties and Standard Measurements of The M16. The detector in this project (M16 scanner) designed by Leddartech company scanner has a 1×16 linear array of 16 segments (horizontal direction - one segment high and 16 segments wide). Each segment acts as a single scanner; each segment works synchronously with the other 15 segments. The physical size of the sensor array, coupled with the optical system results in the sensed area for each segment being 7.5 degrees high and 45 degrees wide, within the wide dimension (45 degrees), there are 16 segments. If the distance between the target and M16 scanner was 1.534 meter then one rectangular segment area will be as follow:

$$\text{Height } 20 \text{ cm} * \text{Width } 7.5 \text{ cm} = 150 \text{ cm}^2 \quad (4.3)$$

From the previous example the formula that can be used to estimate the size of the single segment (Figure 4.11) depending on the distance between the target and the M16 scanner as follow:

$$\text{The segment area in cm}^2 = 0.98 * (X) \tag{4.4}$$

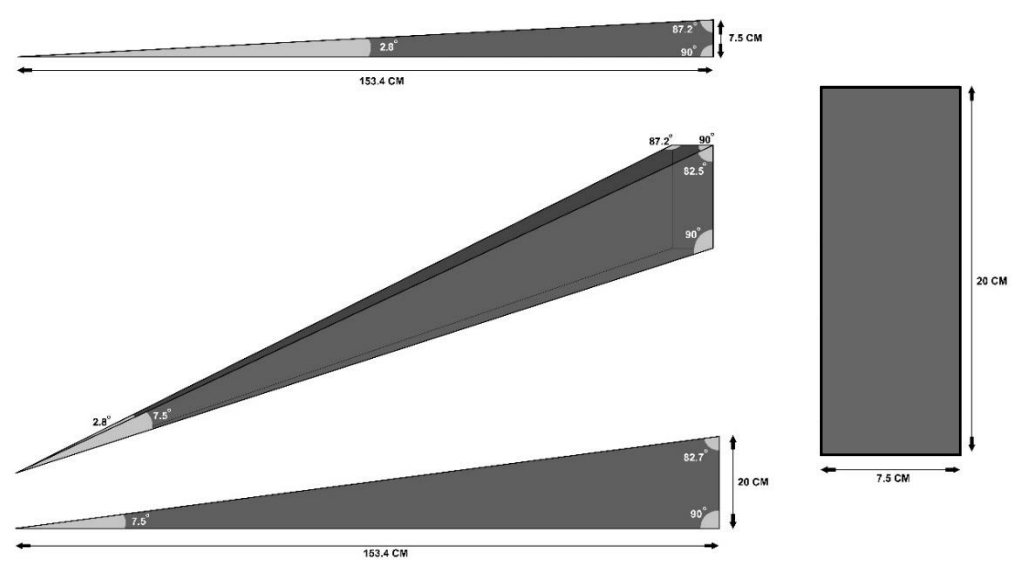


Figure 4.11: Diagram shows one segment dimensions of the M16 sensor beam. The beam aimed at a static target about 153.4 cm away. The single segment width is 7.5 cm, and the height is 20 cm. The vertical angle of the single segment beam is 7.5 degrees, and the horizontal beam angle is 2.8 degrees.

While (X) is the distance between the target and the M16 LIDAR. The full beam width (Figure 4.12) could be calculated by multiplying the width of one segment in the segments number as follow:

$$\text{The full beam width equal} = 7.5 \text{ cm} * 16 = 120 \text{ cm} \tag{4.5}$$

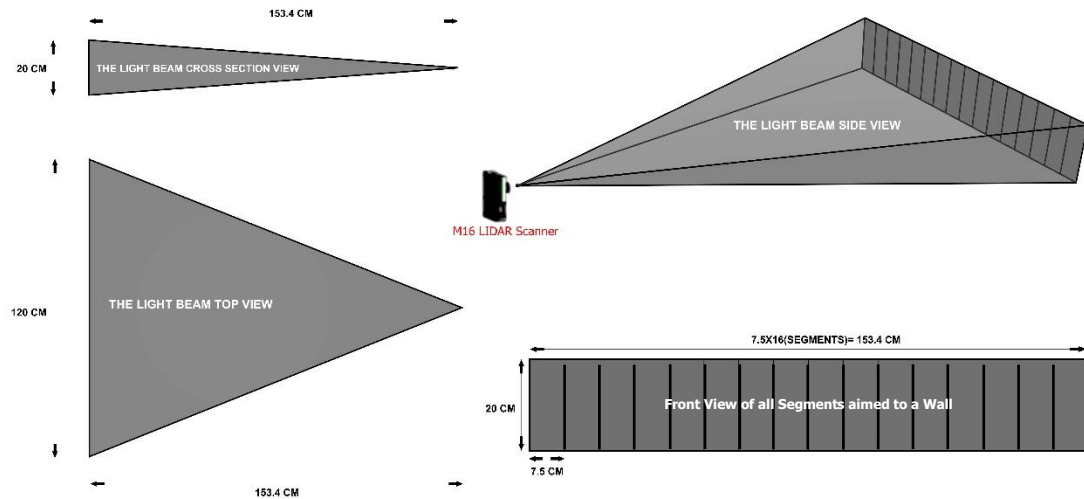


Figure 4.12: The full beam measurements. The height and the width of every single segment when the distance between the target and the M16 scanner is equal to 1.534 meters.

The M16 scanner is light-weight and compact (114 x 76 x 45.3mm, 265g). It consumes around 4W continuous power at 24VDC. The M16 has several M3 machine threads for the mounting purposes, and there is a quarter-20 thread can be used to mount the M16 to a tripod. The light beam width can be customized horizontally to fit the desired detection view from 9°-95° (Bill Gutelius 2014). The LED light is within the infrared band (940 nm), while its pulse rate is typically at 100 kHz. The LED intensity can be customized through the M16 configurator to be automatically or manually controlled. The M16 most important features can be summarized as follow:

- ❖ 16 responsive, independent segments for detecting energy reflected back from the object.
- ❖ 90 to 950 beam view width various options.
- ❖ 0 to 100-meter detection range (325 ft.)
- ❖ Data acquisition rate up to 50 Hz.
- ❖ The accuracy of the detection (of a single measurement) is around 5 cm.

4.4.4 Scanning Protocol with The M16. The communication in the M16 has been done using the serial port (RS-485), or the CAN bus port. Alternatively, the M16 has the USB 2.0 (12 Mbit/s serial port) port which is the easiest method of communication. The RS-485 port on the M16 uses the well-known modbus protocol for the RTU data transmitting mode only.

When sending the detection measurement, one message will be sent followed by messages on ID range to as many as needed in the multiple message mode. The CAN Bus and RS-485 allow the easier integration with any desired application. Communication with the M16 can be done using any choice of the following:

The M16 has one terminal block and contains 8-pins on the top of the M16. It provides CAN, RS-485, besides power connectivity (Figure 4.13). The RS-485 is a half-duplex differential serial port. It is often can be used in electrically noisy environments. The CAN bus is added and can be connected via differential pair wiring.

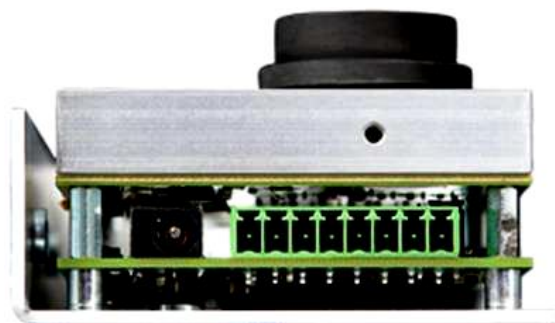


Figure 4.13: M16 scanner power port +RS485 (“Evaluation Kit and Configurator User Guide” 2015).

Pin 2 is used as a power supply to the device directly via the terminal block instead of the DC plug. The ground can be reached through pins 1, 3, and 6. Finally, the RS-485 port can be connected using the pins 4,5, and the CAN bus port can be attached to pins 7,8 Table (4.1).

Table 4.1: Terminal block connector pin definition (“Evaluation Kit and Configurator User Guide” 2015).

Pin	1	2	3	4	5	6	7	8
Function	GND	DCIN	GND	RS-485+	RS-485-	GND	CAN-H	CAN-L

4.4.5 Capturing Raw M16 Measurements. The M16 scanner acquires a base input waveform for each segment in the detection situation at a rate of 12.8 kHz which is under the accumulation 128 and oversampling equal to 8. Multiple acquisitions are made internally, accumulated to provide oversampling and then to generate a final waveform which is processed to produce the distance (“Evaluation Kit and Configurator User Guide” 2015). The final measurement rate can be calculated as follow:

$$\text{Measurement rate} = \text{base rate}/\text{accumulations}/\text{oversampling} \quad (4.6)$$

For example, with 256 accumulations and an oversampling value of 8 then the measurement rate will be as follow:

$$\text{Measurement rate} = 12800 / 256 / 8 = 6.25 \text{ Hz} \quad (4.7)$$

Simply the accumulations can be defined as the number of measurement points that the microcontroller collects and hold before releasing the data set to the processor in the M16 scanner.

Higher values enhance the range, reduce the measurement rate, reduce the noise and the variability. Higher accumulation helps in making the oversampling algorithm process on longer chunks of data, and lower accumulation helps in making the oversampling algorithm process on shorter chunks of data.

Oversampling is a data acquisition channel can help to improve data acquisition by holding the accumulated data set more often and utilizing this collected data to produce one value.

The most straight forward method to produce one value out of the accumulated data is to perform a simple mean average on every accumulated data set.

Oversampling is a process being used in the rebuilding phase of the digital/analog conversion, in which an intermediate high frequency (sampling rate) is used between the digital input/analog output.

Higher values enhance accuracy, precision, resolution, but also reduce the measurement rate. For slow motion, the oversampling should be set to the highest possible value to let the microcontroller collect more data and reduce error and variability.

The accumulation and oversampling help the user to select the setting depending on the object condition. If the user is working on moving objects, then the accumulation should be low and the oversampling as well.

For example in the mine roof monitoring the scanned object is the rock masses which is typically moving very slowly so the user might want to have fewer data points by allowing more of the processing inside the M16 before sending the collected data to the computer.

The base sampling rate is constant and equal to = 12800 Hz, and the highest accumulation is = 1024, and the highest oversampling is = 8. The final sampling rate will be $12800/1024/8 = 1.56$ sample per second after setting the M16 on the previous configuration.

The processing of the collected distance data internally depending on the previous data acquisition configuration will allow the M16 to detect slow objects by outputting fewer data points per second.

On the other hand another example at the field of the autonomous driving. The object here is passing by very fast speed so the user might want to have more data points to detect all objects surrounding the car by doing the processing inside the M16 before sending the collected data to the computer.

Sampling base rate = 12800 Hz , the accumulation = 2 , the oversampling = 2. The final sampling rate will be $12800/2/2 = 3200$ samples per second. Huge anomalies should appear on the collected distance data in this example because of the extreme sampling frequency.

So the manufacturer of the M16 scanner recommends that for the fast objects detecting the sampling frequency might be 100 Hz and 1.56 Hz for detecting slow targets. The following Table (4.2) shows the measurement rate for typical values under a specific number of accumulations and oversampling.

Table 4.2: The measurement rate of the configurator software (“Evaluation Kit and Configurator User Guide” 2015).

Accumulation	Oversampling	Measurement Rate (Hz)
1024	8	1.56
512	8	3.13
256	8	6.25
128	8	12.5
64	8	25
32	8	50
1024	4	3.13
512	4	6.25
256	4	12.5
128	4	25
64	4	50
32	4	100

The accumulation has been used in this project is 1024 and 8 for the oversampling. Any object in the path of the light beam of each segment is captured, measured directly and recorded.

It is qualified by its segment position, its distance, and finally the amplitude, which reflects the returned energy strength from the object that exists in the detection zone. The bigger the light reflection, the higher the amplitude (“Evaluation Kit and Configurator User Guide” 2015). Contrary to collimated emitters (lasers), the M16 scanner LEDs and emitter optics are used to create a diffused beam covering a wider area of interest. The receiver collects the backscatter of the reflected light from objects in the beam and, using full-waveform analysis, detects the presence of objects in each segment of the beam, calculating the distance of the detected objects (based on the time taken by the light to return to the sensor). Accumulation and oversampling techniques are used to maximize range, accuracy, and precision. Sample trace, where the x-axis is a time axis, scaled into the distance, and the y-axis is the light amplitude. The (Figure 4.14) illustrates a typical trace signal for one segment. In this example, the sensor is collecting light reflected back by two separate objects. Full waveform analysis performed by M16 scanner provides the ability to sense multiple targets in the segment. This is possible if the closer object is smaller than the view area for the same segment. The light beam can then illuminate another target that isn’t entirely “shadowed” by the closer target.

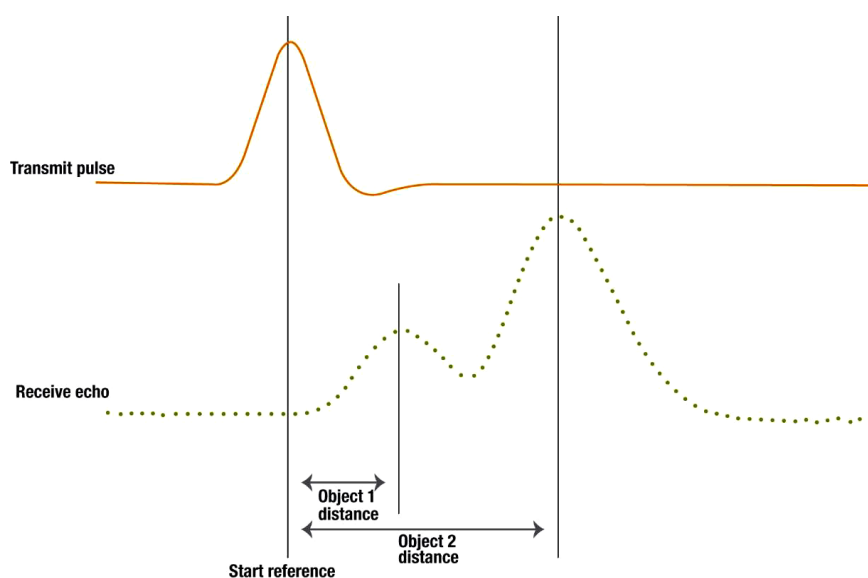


Figure 4.14: The waveform of the reflected energy from the target. This waveform showing two objects has been detected (“Evaluation Kit and Configurator User Guide” 2015).

Depending on the properties of the target's surface, the light signal is either absorbed, totally reflected, or reflected unequally. This causes different irradiances of the echo signal at the receiver, which are measured by the M16 scanner.

This measured irradiance depends on the distance calculated according to the time of flight (ToF) principle of operation and the angle of incidence that can be determined by imaging-collecting optics that focus the reflected beam on the sensor's photodetectors.

It analyzes the resulting discrete time period signal and recovers the distance for every object. M16 scanner light processing can extract the distance for every object found in the field of view. The detection and distance measurements can be visualized by a user-friendly software which can show many details for the detected target (Figure 4.15).

The illumination area and the detection zone has a beam width with 45 degrees (Figure 4.16). The detection and distance measurements are performed by the sensor's processor, using the acquired pulses (one per photodetector).

The pulses consist of a series of values representing light amplitude at incremental distances from the sensor. The number of collected samples in the signal is chosen depending on the maximum range. The amplitude of each sample is an indicator of the amount of light reflected from a given object at that specific distance. The strength of the signal depends on the distance of the target, size, and angle of the target concerning the detector. The target will be detected by the sensor if a light signal above a predetermined threshold is detected.

M16 scanner supporting software sets the default threshold level for every single sensor depending on the signal to noise rate. A threshold table can be applied to the detection analyzing of the traces, and a threshold offset parameter is given on most sensors to adjust this threshold table.

The offset can be set to increase or decrease the sensitivity of the sensor. This can be used to neglect the presence of targets returning the low strength signals or to maximize detection of such targets and filter false detections in the application software.

Another setting available on the M16 scanner is the LED intensity. LED strength control can be set to manual mode or automatic mode. In manual control mode, the setting is regulated by the operator to fit the application best.

In automatic mode, the sensor dynamically will set the LED intensity based on the strength of the signal for objects sensed in the sensor beam.

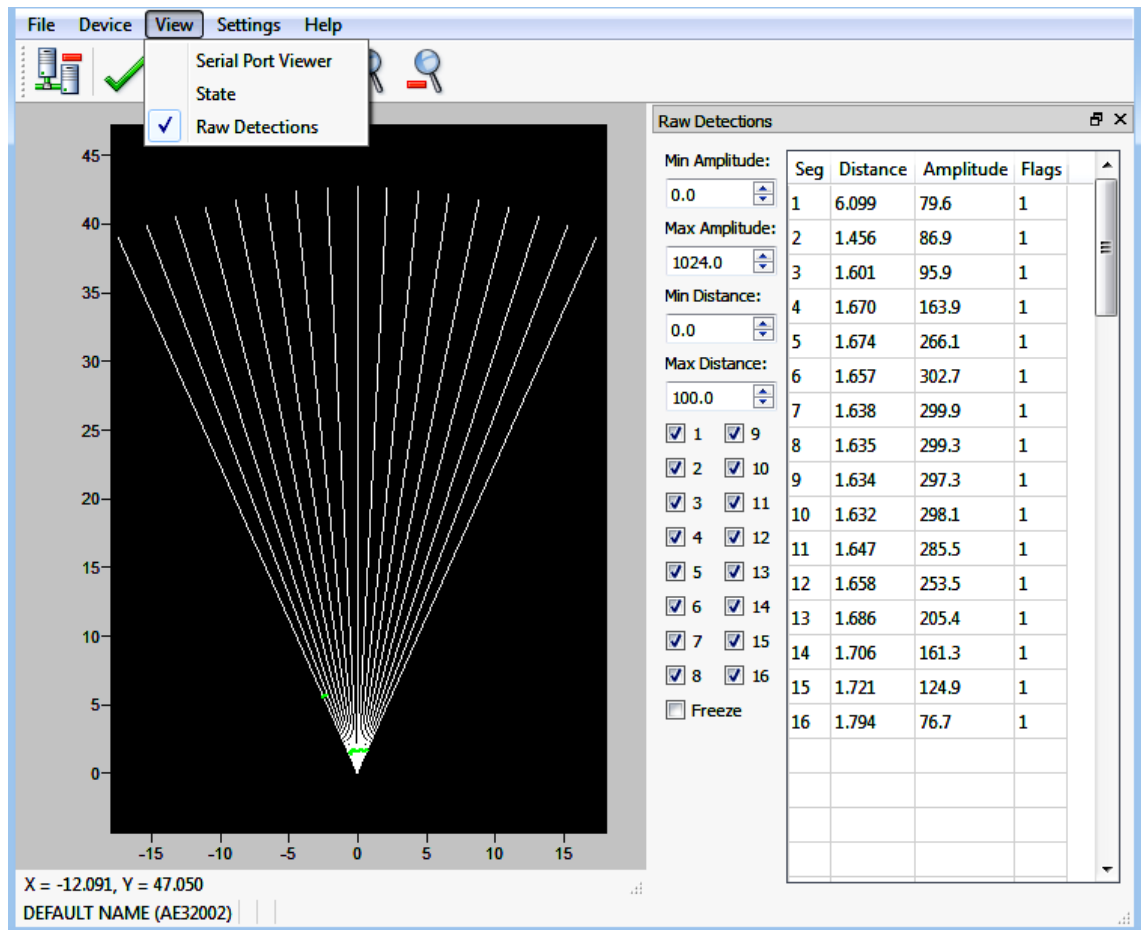


Figure 4.15: Screenshot the main menu of configurator software. The black background section shows the graphical representation of the detected distance, the x-axes in the same section refers to the view size that the lens can cover and the vertical axes refer to the distance of detected objects. The detected objects can be seen in green color, and in this situation, the distance could be estimated to be 1 – 2 meters. The raw detection section gives the user the numerical representation of the detected distance, the amplitude of the reflected light energy (“Evaluation Kit and Configurator User Guide” 2015).

With this control, a detector model can be used for a broad range of applications with different range requirements and can be used in applications where targets can both be very close or far from the detector.

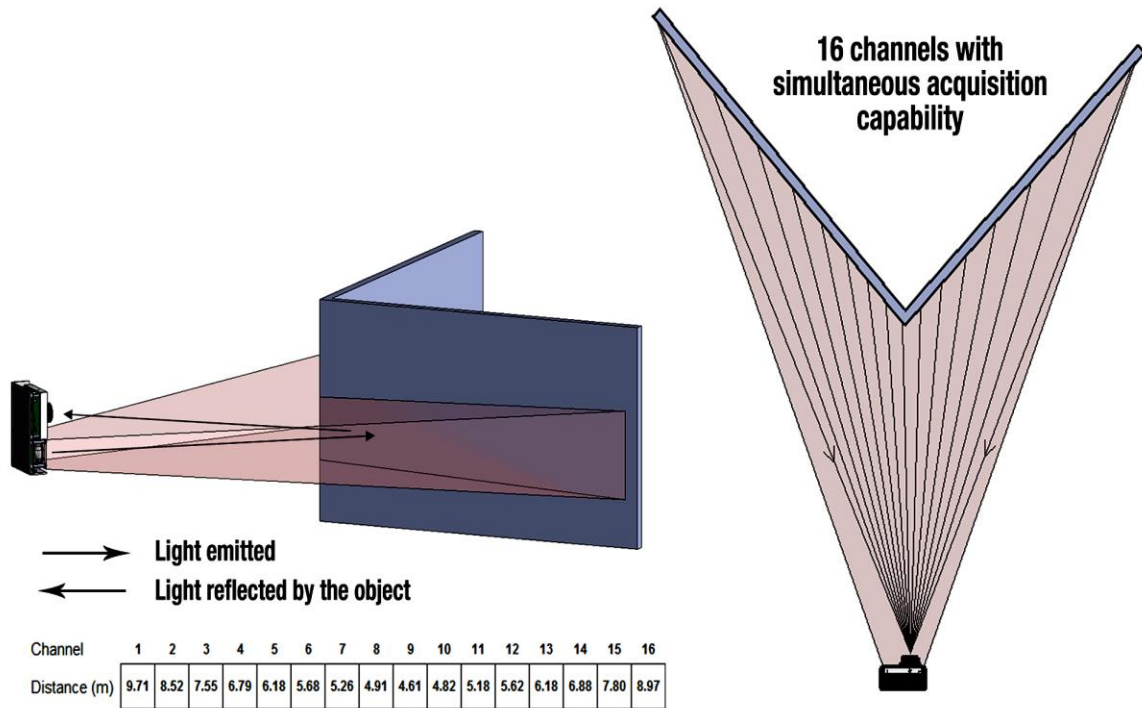


Figure 4.16: Illumination area and the detection zone (“Evaluation Kit and Configurator User Guide” 2015).

The raw detection feature which describes the Segment in which the object is detected, the distance of the object, position (which segment) of the detected object, and the amplitude of light returned from the object and measured by the sensor.

The raw detection feature (Figure 4.17) is one the most important feature which helps to monitor the object detection in the real time and simultaneously with the object movement.

Seg	Distance	Amplitude	Flags
1	6.565	190.9	1
2	1.873	271.9	1
3	1.857	360.8	1
4	1.764	463.3	9
5	1.713	480.7	9
6	1.718	495.9	9
7	1.706	497.3	9
8	1.690	499.7	9
9	1.682	494.3	9
10	1.674	499.4	9
11	1.676	491.6	9
12	1.655	479.9	9
13	1.677	445.2	9
14	1.825	395.3	1
15	1.842	320.1	1
16	1.898	198.1	1

Figure 4.17: Raw detection available feature in the M16 software. (If the flag NO. is 1 this means that the measurement is normal and valid. The saturated signal also is valid if the flag NO. is 9). The freeze parameter freezes the values displayed in the raw detections dialog box. Some segments such as segment NO. 1 have higher values, and this refers that the segments are collecting distance data from the further away object (“Evaluation Kit and Configurator User Guide” 2015).

Trigonometry calculations have been used to determine the optimum size of each segment (in mm - width and height) of the target plate. The distance between the target plate and the sensors. Thus, the detector must be positioned to achieve this optimum segment size on the target plate surface.

It is important to aim the middle 4 segments safely within the lower half of the target plate to avoid the mounting bolt and nut in the center of the target plate (Figure 4.18). These four segments are used to measure the movement of the target plate.

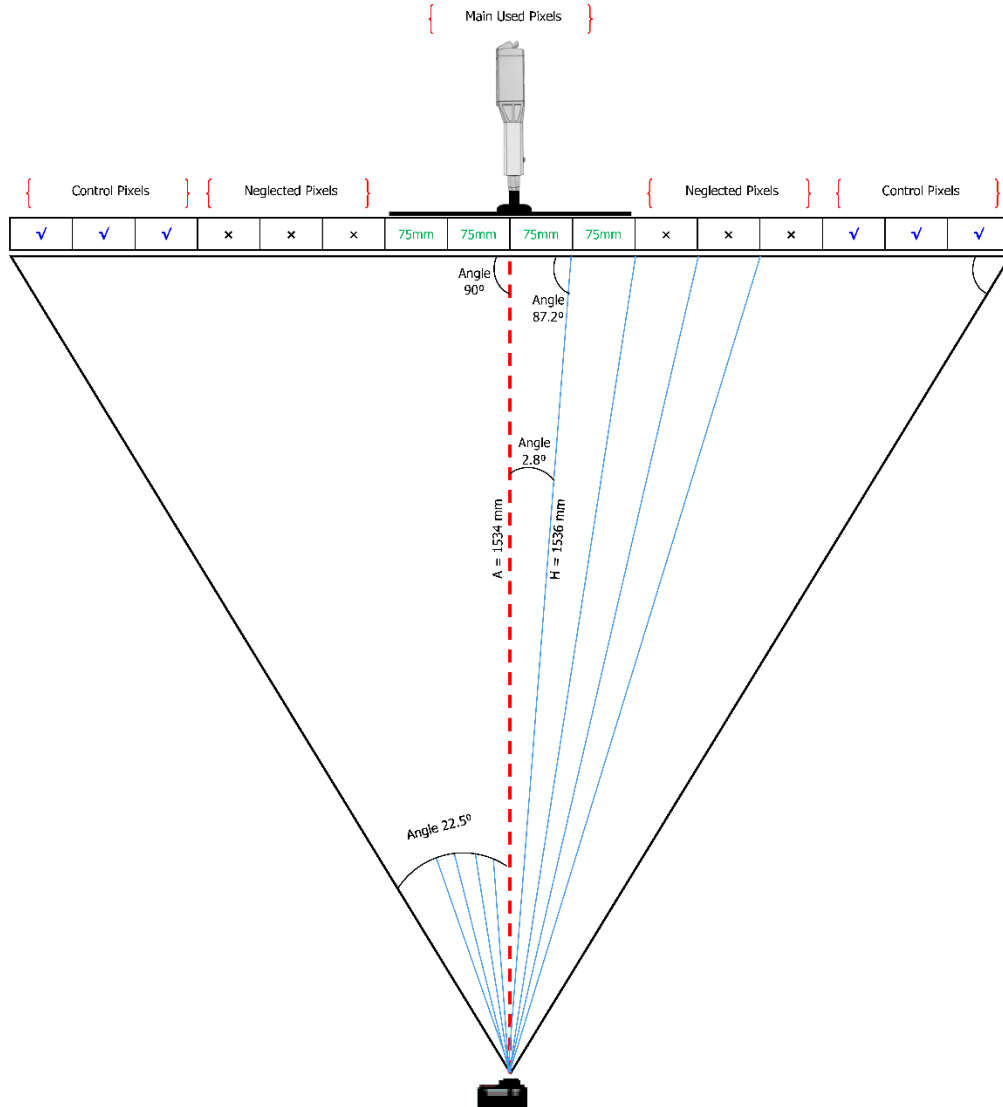


Figure 4.18: The trigonometry calculation between the target and M16 scanner. The trigonometry calculation used to correct the measured distance of outer segments to a perpendicular distance from the target plate so that displacement can be monitored in the direction of the target plate movement.

The sketch above shows that the outer 3 segments on the left and those on the right (6 total) that will be used as control segments - they will be aimed to fall on a static background not connected to the moving target plate.

The rest of the segments (3 on each side from the left and the right) will be neglected as shown in the sketch because 1) they are not needed, and 2) they may or may not partially overlap the moving or stationary target plate. The distance versus time data logging function is used to export the detected data to a .txt format which is capable of being edited.

The .txt file exported can be inserted into any analysis program such as Microsoft Excel, for any statistical purposes. The time stamp of the detected data is shown in the time column.

Each line of the generated text file contains the information related to a single detection Table (4.3). The status of each detection is valid if it is 1, and not valid if it is 9 (“Evaluation Kit and Configurator User Guide” 2015).

Table 4.3: Field description of the log text file (“Evaluation Kit and Configurator User Guide” 2015).

Time (msec)	Segment	Amplitude	Distance (m)	Status
12735204	7	0.9	33.61	1

The time of the detection is 12735204 milliseconds from the time the sensor was started. The location of the detection is segment 7 (the 8th segment). The amplitude of the detection is 0.09, which is very low (small, far, or dark object). The distance of the detection is 33.61 meters. The status of 1 indicates a normal measurement which has been collected, if the value is 9, then the collected data should be saturated.

5 RECTIFYING M16 MEASUREMENTS

5.1 INTRODUCTION TO THE M16 MEASUREMENTS RECTIFICATION

The data which has been collected using the M16 scanner is time series data which means that every observation gathered at a unique point in the timeline of the sampling process. The general definition of the time series data: an ordered sequence of values at a similarly spaced time intervals. The importance of understanding that the data is a data series which is subject to drift that can be best noticed in the raw data, so it is important to take this into consideration while processing or rectifying the data.

Six data sets have been collected to prove the feasibility of using the M16 for detecting roof failures. Three of the collected data sets are under static conditions where there is no movement in the scanning target (target plate). In the case of the other three tests, the M16 is pointed directly at the moving target plate. This test data which has been collected by M16 can be used to answer the question:

Is M16 capable of detecting the movement of the actuator in sub-mm accuracy? If so then it can be used to monitor and detect the roof failures in mines ?. The data has been collected can be summarized in the following Table (5.1):

Table 5.1: The test NO. versus test type (Dynamic/Static).

Test NO.	Type (Dynamic/Static)	Reason
1 D	Dynamic	To Explore the precision that M16 can provide for detecting a moving target.
2 D	Dynamic	
3 D	Dynamic	
1 S	Static	To explore the drift behavior.
2 S	Static	
3 S	Static	

5.2 PROBLEMS AND SOLUTIONS

This project countered many obstacles and the proper solution should be used to avoid any delay in collecting the data or even collecting the data including the anomalies which will cause the wrong interpretation.

5.2.1 Zero Offset Effect. The M16 basically is a device that measures the distance to the scanned object, so the zero point of the movement detection is the distance measured at the beginning of the sampling process.

The scan progressing has been split out into various parts; the first part has been considered as the baseline that will be helpful to detect the drift in the static measurements and act as the zero point that can also be a method to measure the displacement.

5.2.2 Environmental Variables Affecting the Scanning Results. The research time limit prevents the author from exploring all possible environmental effects on the collected data such as Temperature, external and internal to the M16.

- ❖ Humidity.
- ❖ Dust.
- ❖ Vibration.

However, one solution was discovered while collecting the data. That was to ensure that the temperature of the scanner while collecting data is at room temperature. For the current test, there's little excess humidity and no dust in the environment that has been used for testing.

In order to keep as many variables the same, the same cables were used in every single test. The test was conducted in a quiet area far away from any vibration sources such as classrooms which typically have many activities.

5.2.3 Drift Effect. Drift with time is one of the biggest problems that were encountered. Unfortunately, measuring the signals through M16 is not always as accurate as other expensive LIDAR machines.

Understanding the temperature effect on the distance collected data will be the very effective solution for the drift over time. The external temperature of the environment and the internal temperature of the M16 are the main reason for distance

data drifting over time. It is difficult to collect precise and noiseless data, but it is possible to do extensive filtering to have much more accurate final results.

5.2.4 M16 Settings Effect. The M16 data acquisition settings such as the accumulation and oversampling have to be set before every single test. The problem is that those settings are affecting the final collected raw distance data by making the raw data noisy if the sampling rate is high. It is possible to choose the lowest sampling rate for detecting the target plate displacement, but also this means that the collected data points will be very few and not suitable for the rectification processing which needs a huge data points to apply the outliers detection and remove the anomalies; therefore averaging all the remain data points. If the data acquisition settings of the M16 scanning tool impact on the output has been understood to this project, it might be easier to stick with standard setting, but unfortunately, the relationship between the output data and the data acquisition settings in this project environment are not specified yet.

5.2.5 Segments Position Effects. Because of the different angle of each of the segments reflecting off a planar surface, every segment measures a different distance from a planar target. The expected result is that every segment detected the distance of the object differently (Figure 5.1).

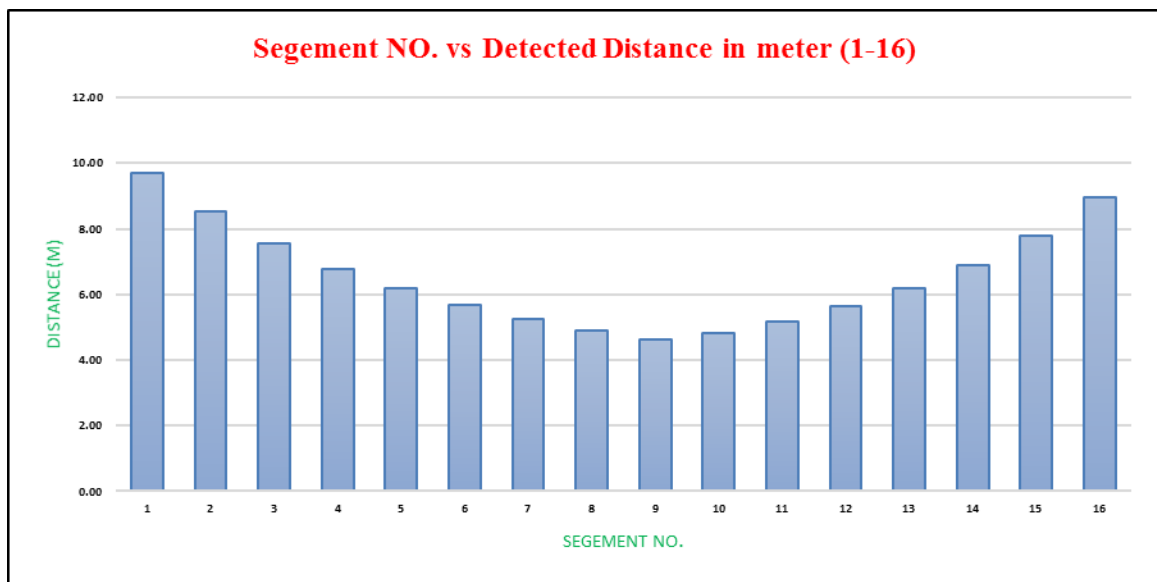


Figure 5.1: All 16 segments aimed at the same planar target. The beam gives different distance results as a result of the different distances to the target.

5.2.6 Electrical Components Instability. Electrical components might be a principal reason for the instability of measurements. The most critical component that might be causing any disturbance to the collect distance data is the power supplier. The fluctuation and the instability of the provided power in any electrical device, and this may be one reason that causes the noisy distance data in the M16 scanner.

5.2.7 M16 Internal Temperature Effect. The M16 internal temperature is most likely increase the longer the machine is functioning. This temperature increase can be easily noticed by touching the outer aluminum frame. The internal temperature increasing with time and might be one reason of the drift over time.

5.2.8 The Target Plate Material Effect. The target plate attached to the actuator basically made of thin steel so the elastic behavior of the steel might be introducing some variability to the results due to the instability of the target plate while the actuator is driving it. The ground vibration is one major expected reason that might be making the target plate not stable. The other minor reason might be the air current which can be coming from the surrounding appliance such as the air conditioner or even opened windows. The recommended target plate has to be made from thick material to get much more accurate results. If the target plate is solid and heavy, this means more resistant to the elastic behavior and more stable during the target plate travels from the static condition to the moving condition when moving the target plate. It would be beneficial if the target plate manufactured from a thicker material as this will make the simulation of the roof failure less variable and would resist movement in response to the air current.

5.3 DATA RECTIFICATION TECHNIQUES

The collected data has a considerable number of outliers, so it is very important to correct the collected data. Without correcting the data has been collected, it might be no benefits to using the M16 scanner in sub-mm applications. So in order to produce a valuable displacement data then it's needed to remove the drift in collected distance data due to the temperature and do the rectification using some widely-accepted methods.

5.3.1 Introduction to the Rectification Techniques.

The rectification will be done in equal time periods named (integration periods). The integration periods is that equal period which the processing of the outliers detection

and removing can be done through it. The integration period which is used in this thesis is 30 seconds, which means the processing of the outliers detection and removing will be done in every 30 seconds.

5.3.2 IQR. The interquartile range (IQR) (Figure 5.2) is a measure of variability, based on dividing a data set into quartiles. Quartiles split a rank-ordered data set into four equal parts. The values that divide each part are called the first, middle, and last quartiles; and they are referred by Q1, Q2, and Q3, as follow (Tukey 1977):

- ❖ Q1 relates to the "middle" value in the first half of the ordered data group.
- ❖ Q2 refers to the median value ordered data group.
- ❖ Q3 refers to the "middle" value in the last half of the ordered data group.

The IQR the result of subtracting the "middle" value in the last half of the ordered data group (Q3) and the "middle" value in the first half of the ordered data group (Q1) (Tukey 1977). The IQR range is the center 50% of a data group.

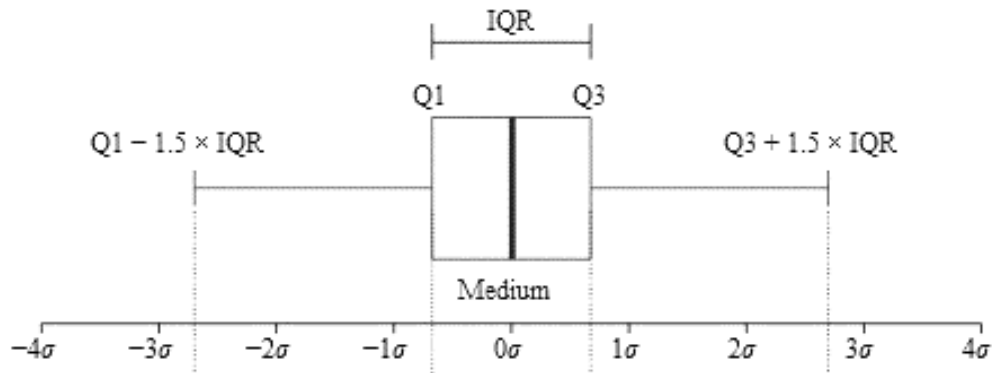


Figure 5.2: Interquartile range box and whiskers plot.

The method of interquartile range (IQR) can efficiently remove the major percentage of the outliers. It's very effective statistics technique and extensively used for these type of rectification.

5.3.3 Z-Score. A Z-score: indicates how many standard deviations (σ) from the mean. The standard z-score is calculated from the following equation:

$$z = (X - \mu) / \sigma \quad (5.1)$$

Where z is the standard z-score, X is the value of the item, μ is the population arithmetic mean, and (σ) is referred to the standard deviation of the data group (HELM Learning Technologist 2004). The z-score along with the normal can be used to give a visual representation of the distribution of the collected data in a reverse bell shape. The z-score can be used to cut off the tails of the normal distribution reverse bell shape. It is very effective way to remove the outliers placed on the edges of collected distance data (Figure 5.3).

By cutting off the z-score of the data points that have a Z-score than 1.5, and do the same thing with the data points that have a Z-score less than -1.5. The collected data will be effectively cleaned from another major percentage of the outliers.

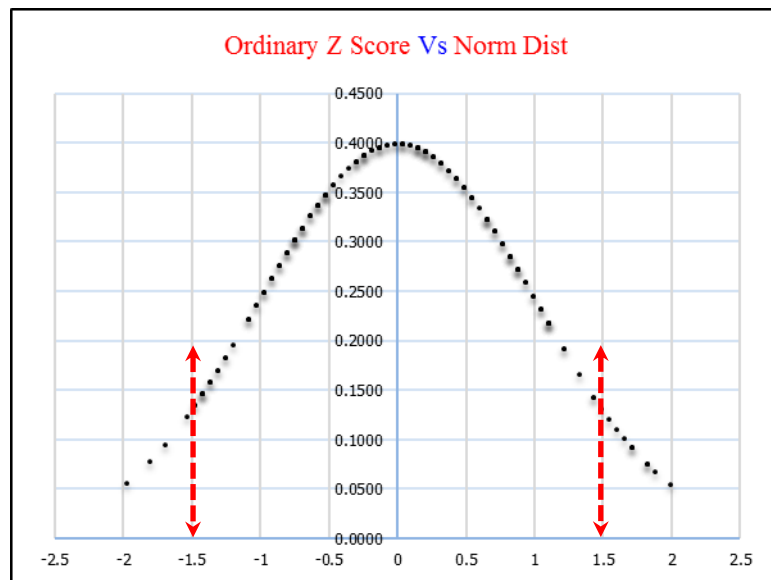


Figure 5.3: The z-score used to cut off the tails of the distance collected data. The red arrows show the starting point of the curve tails truncation.

5.3.4 Drift Correction. The drift correction can be done by collecting two types of distance data points. The static data points group is the first one and the second one is the dynamic or displacement data group. To apply the drift correction using this method, the two data group should be collected simultaneously without any time shifting in the data. Fortunately, there is no time shifting in the distance data collected by the M16 scanner, and the is one advantage of the M16 scanner which is collecting the data of all segments together at the same time. The only thing it has to be done is to assure that the segment of which responsible for detecting the static target should not by any chance collide with any moving object. Then after getting the two data points one for the static object and the other for the moving object, the drift should be measured over time. Finally, it will be easy to subtract the drift has been measured in the static data points from the dynamic data points. The data group that should be collected can be summarized as follow:

5.3.4.1 Dynamic segment NO. 9. (for detecting movements). The segment number 9 is in the middle segment and has been positioned at a vertical angle to the target plate. It has been chosen to be the displacement measuring sensor. This segment has been chosen to collect the dynamic data group.

5.3.4.2 Static segment NO. 16. (for measuring the drift). The segment number 16 has been used with the segment number 9 in order to measure the drift. The segment NO. 16 will be aimed at a static target in order to collect distance data and lastly to calculate the drift over time. Segment NO. 16 has been chosen because it has the least chance of hitting the moving target so it can be used to detect the drift over time. Segment number is used as the reference segment. This segment has been chosen to collect the static data group.

5.3.5 Averaging. An arithmetic mean is an average rating, often denoted by X . It is the sum of every single score divided by the number of the data set. Thus, if there is a group of N numbers (X_1, X_2, \dots, X_N), the arithmetic mean of those items would be determined as:

$$X = (X_1 + X_2 + \dots + X_N) / N = [\sum X_i] / N \quad (5.2)$$

5.3.6 Moving Average. A moving average is a well-known method used with data time series which used to smooth out the short-term fluctuations of the data sets and highlight the long-term data sets trend. The threshold between short and long-term depends on the application, and the parameters of the moving average will be set accordingly.

Moving average: is a type of convolution, in other words, it can be viewed as an example of the low-pass filter which is used commonly in signal processing. Is calculated by taking the arithmetic mean of a given set of values. The moving average is a calculation to processed data set by creating multiple series of arithmetic means of different subgroups of the full data points. The moving average can be described simplistically as smoothing processing to the data set; the moving average would be determined as:

$$M_t = (X_t + X_{t-1} + \dots + X_{t-N+1}) / N. \quad (5.3)$$

The forward-looking moving average is a technical analysis tool that allows the users to smooth out the past data to generate trend-following indicators. Simple moving averaging does not allow future prediction.

So when the simple moving average is predicting the future data behavior, then it is called as forward moving average. Forward moving average required to wait a small amount of time to calculate for a given time. The waiting time in forward moving average means that it's needed to collect more data points, therefore start the processing of forward moving average.

Backward-looking moving average: is a technical analysis tool that allows the users to smooth out the data to generate trend but it is not a trend-following indicator. The simple moving averaging do not allow the future prediction. A backward moving average can be done in real time.

Simple moving average (SMA) is a running arithmetic moving average used to smooth a data series. Short-term averages respond quickly to changes in the data of the underlying, while long-term averages are slow to react.

Displaced moving average is a moving average that has been time-shifted either forward or backward. Displaced moving averages are constructed by taking the moving average and shifting it by a number of intervals, either positive or negative.

Forward moving average (Figure 5.4) if the shifting by a positive intervals number, then the displaced moving average will lag the original moving average. Backward moving average (Figure 5.5) if the shifting by a negative intervals number, then the displaced moving average will lag the original moving average.



Figure 5.4: Forward moving average. The forward moving average means that data can be used to predict the future events.



Figure 5.5: Backward moving average. The backward moving average means that data cannot be used to predict the future events.

6 DATA RESULTS, AND INTERPRETATION

6.1 STATIC TESTS AND RESULTS

The static test is conducted by aiming the M16 scanner scanning to a static planar target that will not move while scanning. The test outputs will include the distance data between the static object and the M16 along with its collection time. The static test will help to understand the drift which might occur in the collected distance data by the M16.

6.2 RAW DATA OF THE STATIC TESTS VS. RECTIFIED DATA

The raw data in this section has many spikes. There are many reasons for the cause the presence of spikes in the distance collected data. The most possible cause of the mentioned outliers is the temperature (internal temperature of the M16 and external temperature of the outside environment).

The main purpose of using the rectification techniques is to remove the anomalies that might be one reason makes the interpretation process harder. The outliers detection techniques have been used successfully to remove most of the anomalies and outliers in the distance collected data by M16 LIDAR.

The static tests (Figures 6.1 – 6.6) have been done to understand the drift behavior of all 16 segments while aiming the segments directly to a motionless target plate. The moving average that has been done on the raw static tests data makes the rectified data drift with time depending on the temperature change higher than the raw data due to averaging the downward noise with the upward noise Table (6.1 – 6.6).

The moving average should not be used to calculate the drift; it is beneficial for doing the data graphs much more distinctive from each other. The moving average only makes the static test data much more clear to differentiate and compare.

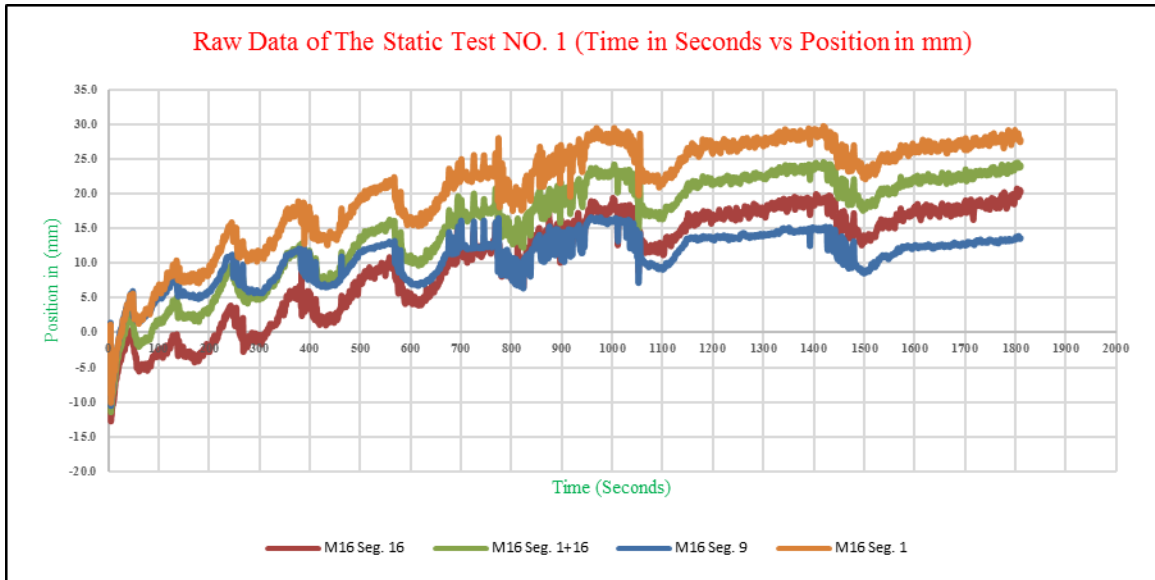


Figure 6.1: Raw data of the static test NO. 1.

Table 6.1: The maximum drift of raw data of the static test NO. 1.

	Seg. 1 Drift without rectification	Seg. 9 Drift without rectification	Seg. 16 Drift without rectification	Seg. 1+16 Drift without rectification
Max	29.75	16.62	20.75	24.56

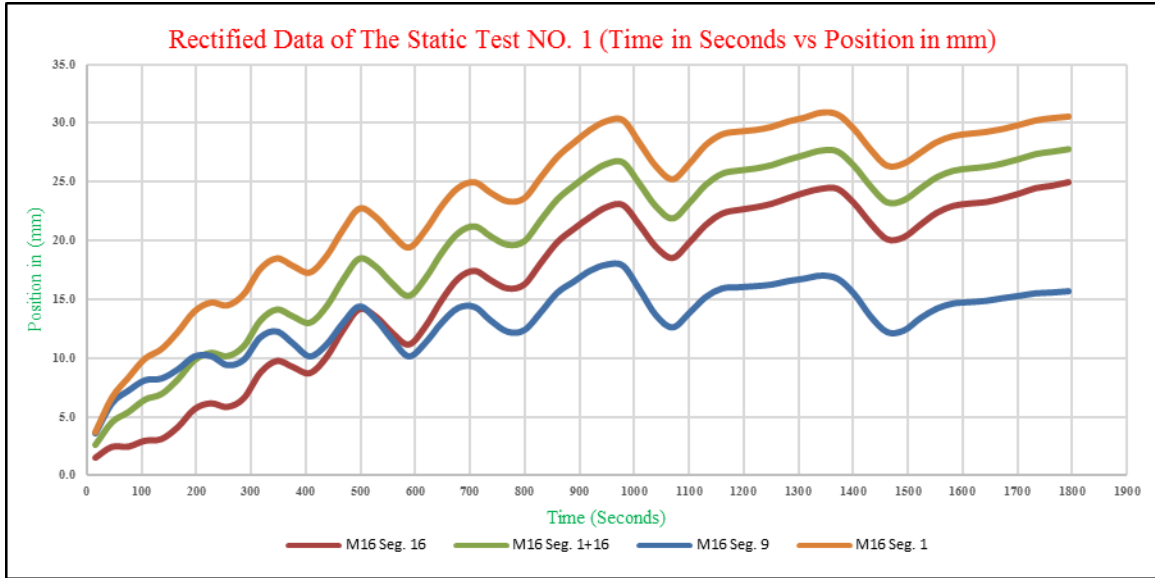


Figure 6.2: Rectified data of the static test NO. 1. (The rectification including the IQR processing, Z-score processing, simple averaging, and finally moving average).

Table 6.2: The maximum drift of rectified data of the static test NO. 1.

	Seg. 1 Drift with rectification	Seg. 9 Drift with rectification	Seg. 16 Drift with rectification	Seg. 1+16 Drift with rectification
Max	30.92	17.98	24.97	27.78

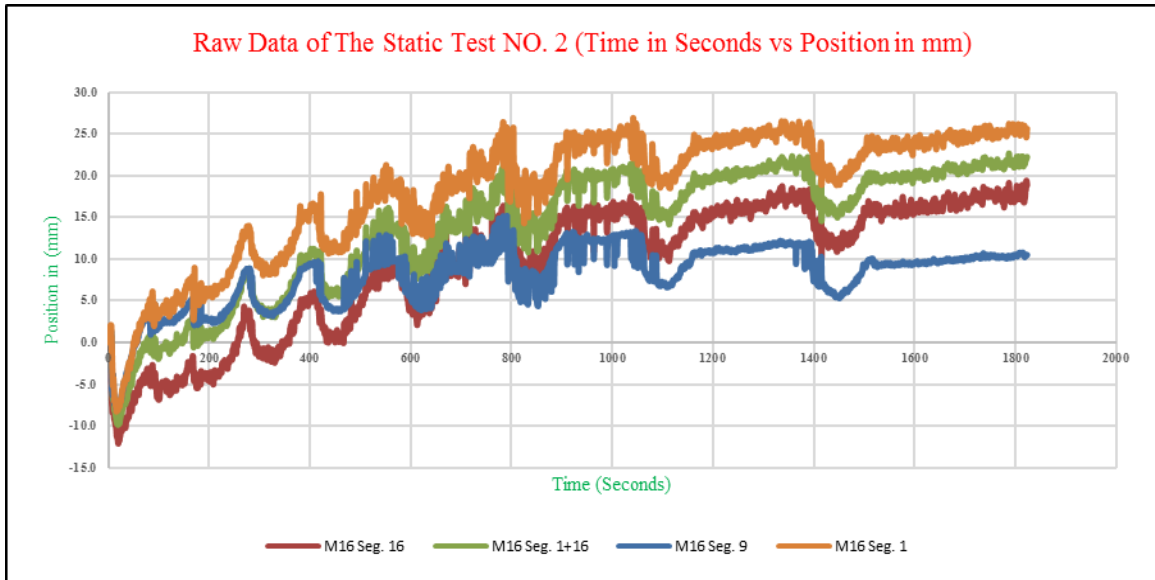


Figure 6.3: Raw data of the static test NO. 2.

Table 6.3: The maximum drift of raw data of the static test NO. 2.

	Seg. 1 Drift without rectification	Seg. 9 Drift without rectification	Seg. 16 Drift without rectification	Seg. 1+16 Drift without rectification
Max	26.86	15.17	19.38	22.66

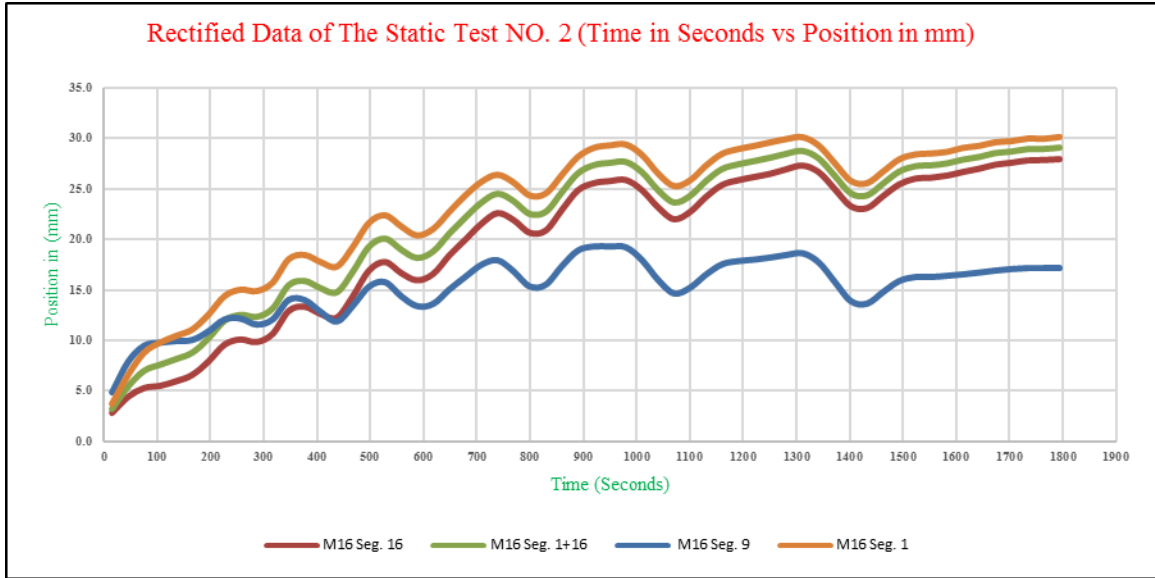


Figure 6.4: Rectified data of the static test NO. 2. (The rectification including the IQR processing, Z-score processing, simple averaging, and finally moving average).

Table 6.4: The maximum drift of rectified data of the static test NO. 2.

	Seg. 1 Drift with rectification	Seg. 9 Drift with rectification	Seg. 16 Drift with rectification	Seg. 1+16 Drift with rectification
Max	30.16	19.30	27.94	29.05

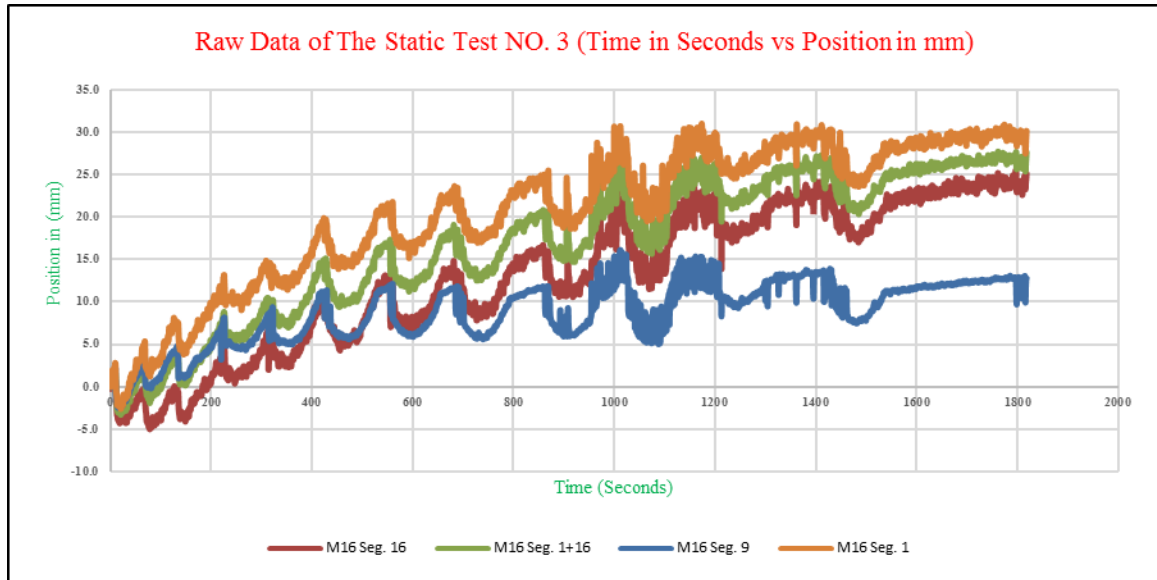


Figure 6.5: Raw data of the static test NO. 3.

Table 6.5: The maximum drift of raw data of the static test NO. 3.

	Seg. 1 Drift without rectification	Seg. 9 Drift without rectification	Seg. 16 Drift without rectification	Seg. 1+16 Drift without rectification
Max	30.96	16.10	25.51	27.68

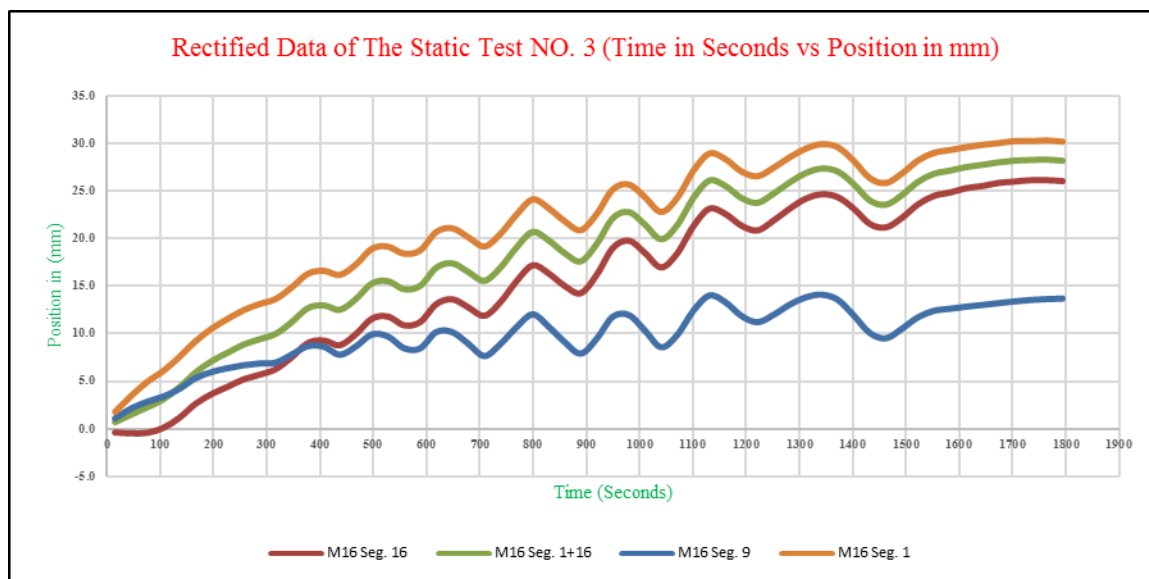


Figure 6.6: Rectified data of the static test NO. 3. (The rectification including the IQR processing, Z-score processing, simple averaging, and finally moving average).

Table 6.6: The maximum drift of rectified data of the static test NO. 3.

	Seg. 1 Drift with rectification	Seg. 9 Drift with rectification	Seg. 16 Drift with rectification	Seg. 1+16 Drift with rectification
Max	30.27	14.15	26.15	28.21

6.3 DYNAMIC TESTS AND RESULTS

Three movement profiles (Figures 6.7 - 6.9) have been created to test the M16 ability in detecting the movement; these artificial profiles Table (6.7 – 6.9) are projected to move the target plate, while the M16 is aimed directly at the target plate and collecting the data. The maximum movement of every single artificial profile is shown in the Table (6.10).

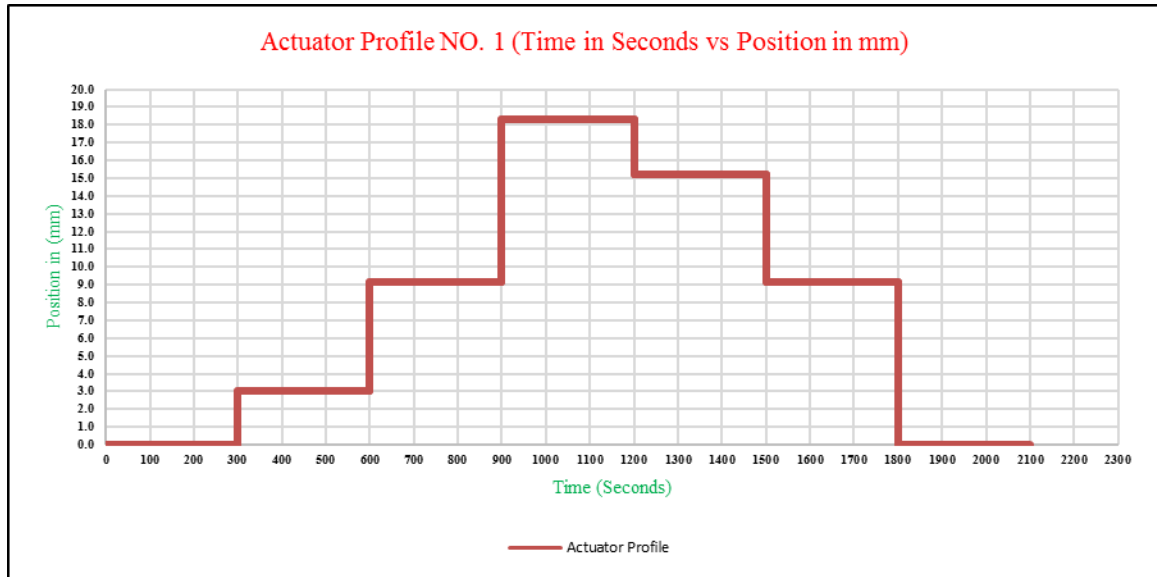


Figure 6.7: Actuator profile NO. 1.

Table 6.7: Actuator profile NO. 1.

X Time in Seconds	Y Position in mm
0	0
300	0
300	3.048
600	3.048
600	9.144
900	9.144
900	18.288
1200	18.288
1200	15.24
1500	15.24
1500	9.144
1800	9.144
1800	0
2100	0

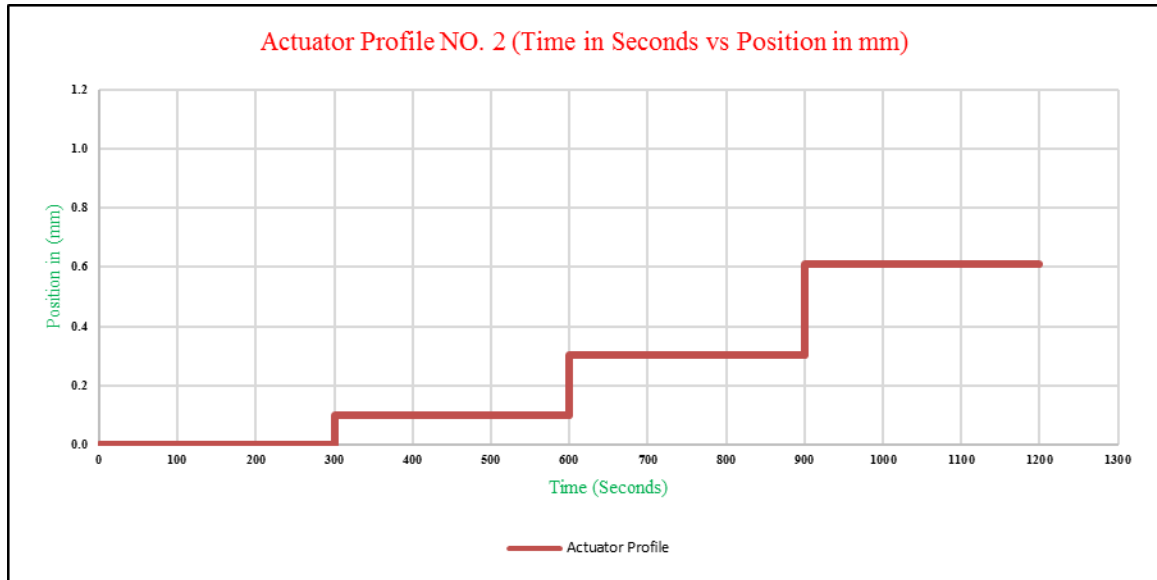


Figure 6.8: Actuator profile NO. 2.

Table 6.8: Actuator profile NO. 2.

X Time in Seconds	Y Position in mm
0	0
300	0
300	0.1016
600	0.1016
600	0.3048
900	0.3048
900	0.6096
1200	0.6096

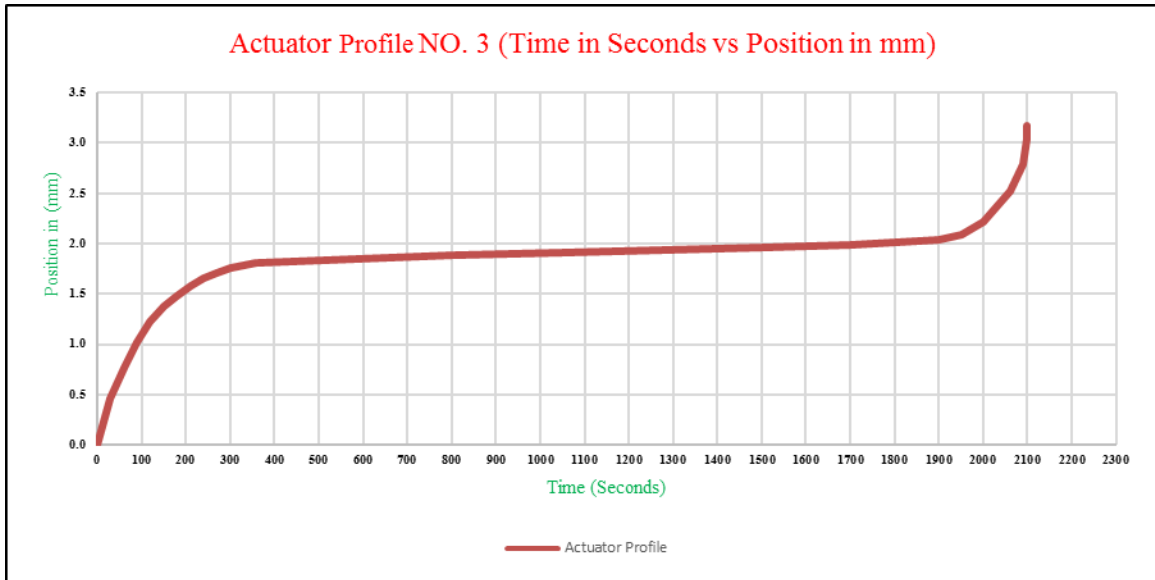


Figure 6.9: Actuator profile NO. 3.

Table 6.9: Actuator profile NO. 3.

X Time in Seconds	Y Position in mm
30	0.4572
60	0.762
90	1.016
120	1.2192
150	1.3716
180	1.4732
210	1.5748
240	1.651
270	1.7018
300	1.7526
330	1.778
360	1.8034
800	1.8796
1050	1.905
1500	1.9558
1700	1.9812
1900	2.032
1950	2.0828
2000	2.2098
2060	2.5146
2090	2.794
2100	3.048

A laser pointer has been installed in the middle of the upper edge of the M16 scanner. The laser pointer installed in order to set the M16 scanner perpendicularly with target plate every single time the experiment needs to be performed. Also, the importance of the laser points is to assure that the M16 scanner has the middle position of the target plate before testing (Figure 6.10).

Table 6.10: Scan duration and maximum movement of every single test.

NO.	Test	Scan Duration (Sec.)	Actuator Profile NO.	Max Displacement (mm)
1	1D	2100	Actuator Profiles NO. 1	18.288
2	2D	1200	Actuator Profiles NO. 2	0.6096
3	3D	2100	Actuator Profiles NO. 3	3.175

The dynamic tests have been done to understand the M16 ability to track the target plate and detect the amount of movement. The fourth middle segments have been used to detect the movement while aiming the segments directly to a “target plate” object while the other segments aimed to a fixed object to subtract the drift which occurs in the measurement.

This test will show the M16’s ability to detect small movements. The only segment NO. 9 is used to detect the movement and the only segment NO. 16 segment is used to detect the drift.

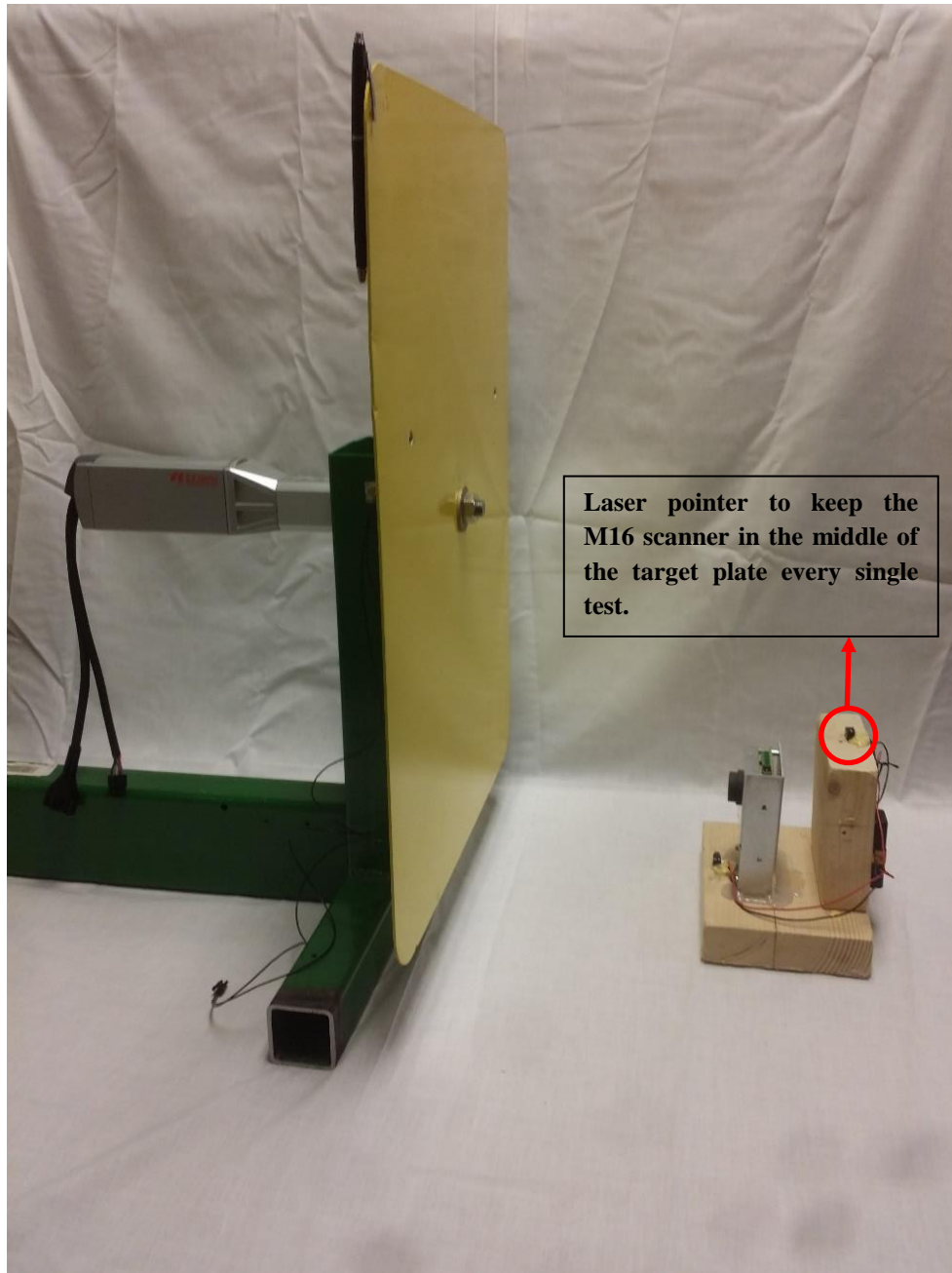


Figure 6.10: To detect the target plate accurately, the M16 scanner light beam. The light beam should be aimed perpendicularly to the target plate with no inclination angle.

6.4 RAW DATA OF THE DYNAMIC TESTS VS. RECTIFIED DATA

(Figures 6.11 – 6.16) show that the raw detected data is following the actuator profile and tracking the same pattern, with limited success because of the anomalies, noise, and outliers.

The rectification has been done to the data besides additional statistical enhancement has been applied which makes the measurements much more clear for comparing purposes. The rectification has been mentioned at the beginning of this section. The final results of every single dynamic test correspondence to the actuator profile is shown in the Table (6.11 – 6.13)

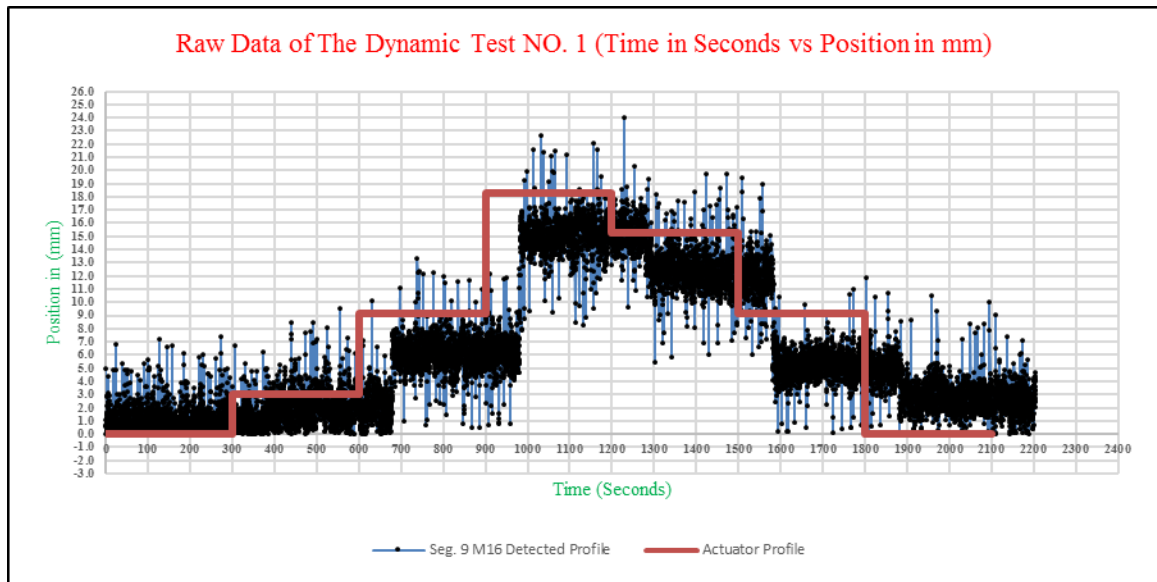


Figure 6.11: Raw data of the dynamic test NO. 1. The red line shows the actual displacement.

In test NO. 1, the detected profile noticeably follows the actuator profile. The green dot is sitting in the middle of every step period and denotes reading on each profile (actuator profile and detected profile). Thus it is possible to compare the detected profile green dot to the green dot of the actuator profile.

The Table (6.11) shows the reading of the green dot of the detected profile versus the green dot of the actuator profile and the difference between both the two readings.

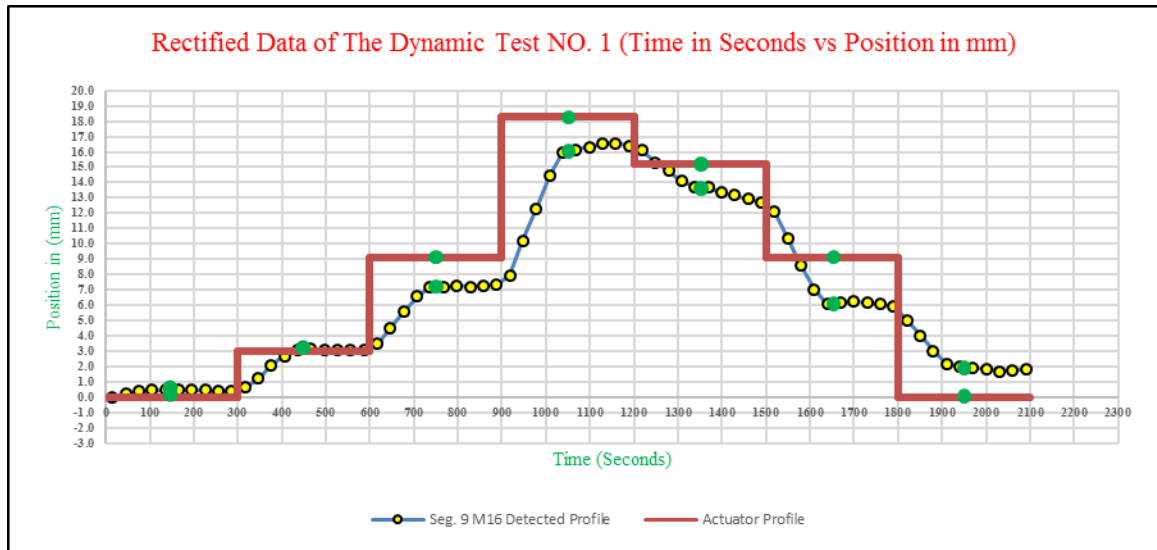


Figure 6.12: Rectified data of the dynamic test NO. 1. The figure after the interquartile range (IQR) plus the moving average have been used. The red line shows the actual displacement. (The rectification including the IQR processing, Z-score processing, drift correction, simple averaging, and finally moving average).

Table 6.11: Actuator vs. the detected profile the rectified dynamic test NO. 1 data.

Test NO. 1		
Actuator Profile (mm)	Detected Profile (mm)	Error (mm)
0	0.5	0.5
3	3	0
9	7	2
18	16	2
15	13.9	1.1
9	6	3
0	2	2

Simply the most two things can be noticed from the test NO. 1 is the error of (vertical distance between the two green dots beside the reaction time which is half the length of each stage).

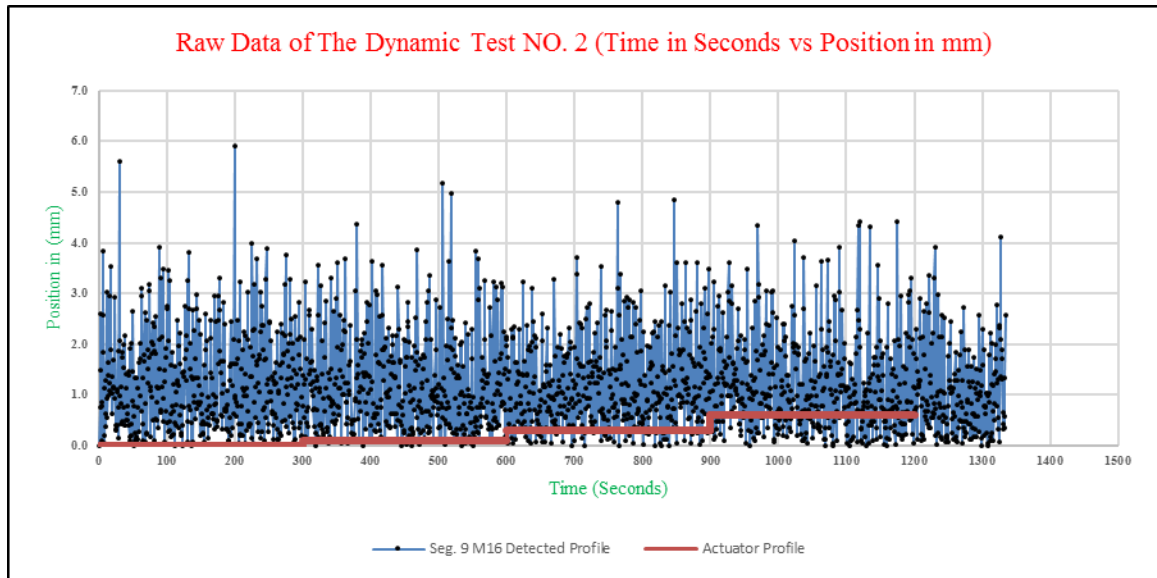


Figure 6.13: Raw data of the dynamic test NO. 2.

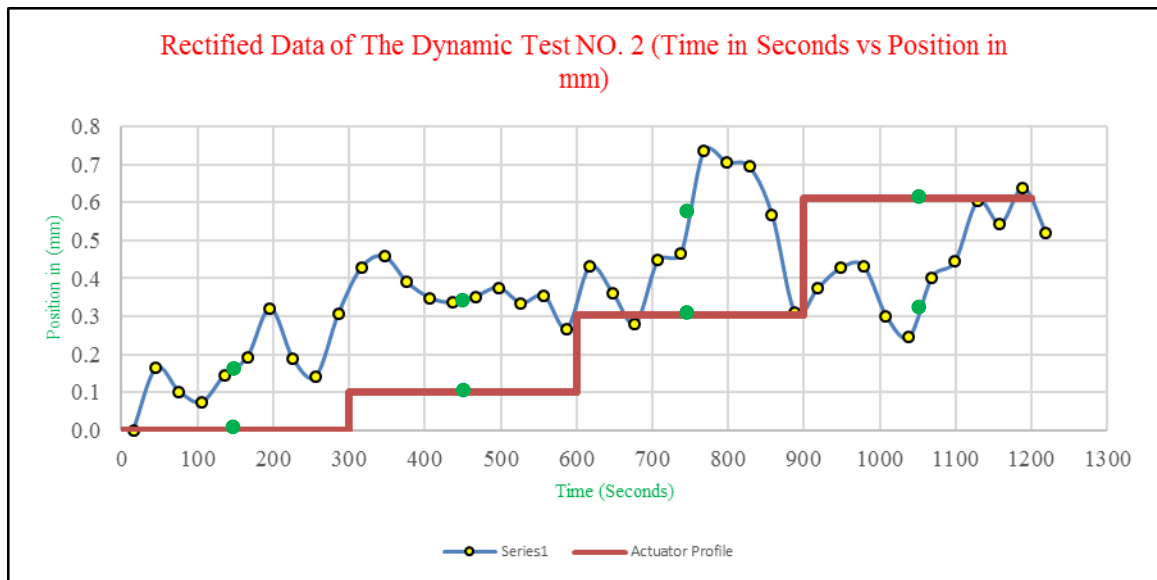


Figure 6.14: Rectified data of the dynamic test NO. 2. (The rectification including the IQR processing, Z-score processing, drift correction, simple averaging, and finally moving average).

In test NO. 2, the detected profile is considerably following the actuator profile if the data collection started from the same point that the actuator has begun from. The green dot is set in the middle of every step period and denotes reading on each profile (reading of the actuator profile or reading of the detected profile).

It is possible to compare the detected profile green dot to the green dot of the red actuator profile because of the two green dots has been placed in the same time region. The Table (6.12) shows the reading of the green dot of the detected profile versus the green dot of the actuator profile and the difference between both the two readings. Simply the most two things can be noticed from the test NO. 2 is the error of (vertical distance between the two green dots beside the reaction time which is half the length of each stage).

Table 6.12: Actuator vs. the detected profile of the rectified dynamic test NO. 2 data.

Test NO. 2		
Actuator Profile (mm)	Detected Profile (mm)	Absolute Precision
0	0.19	0.19
0.1	0.35	0.25
0.3	0.55	0.25
0.6	0.32	0.28

In test NO. 3, the detected profile is following the actuator profile. The green dot is set in the middle of every step period and denotes reading on each profile (reading of the actuator profile or reading of the detected profile). It is possible to compare the detected profile green dot to the green dot of the red actuator profile because of the two green dots has been placed in the same time region. The Table (6.13) shows the reading of the green dot of the detected profile versus the green dot of the actuator profile and the difference between both the two readings.

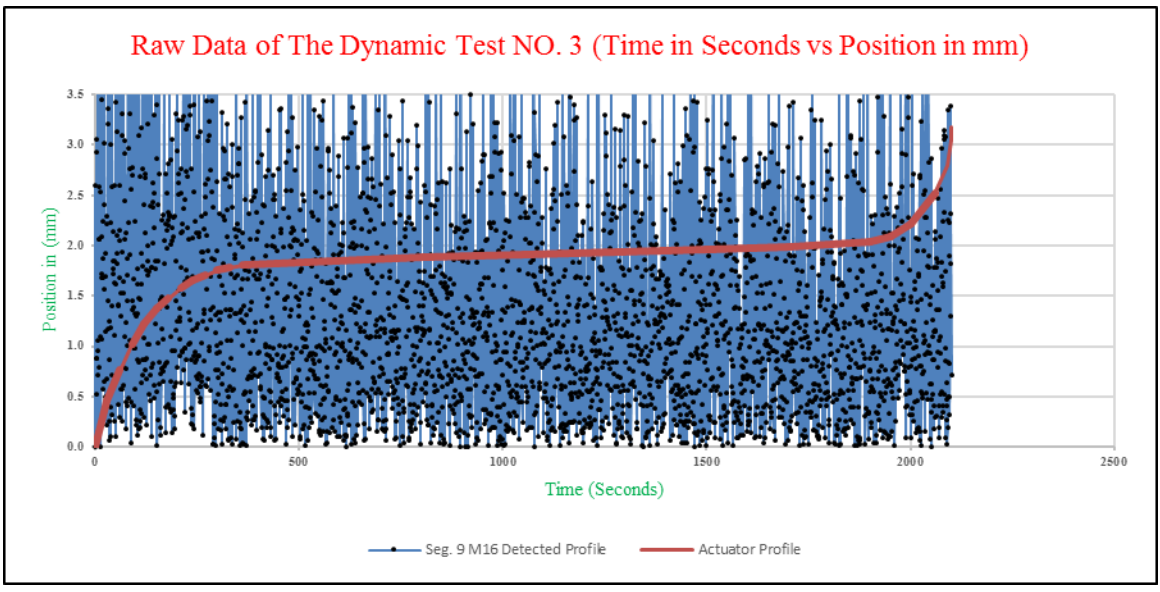


Figure 6.15: Raw data of the dynamic test NO. 3.

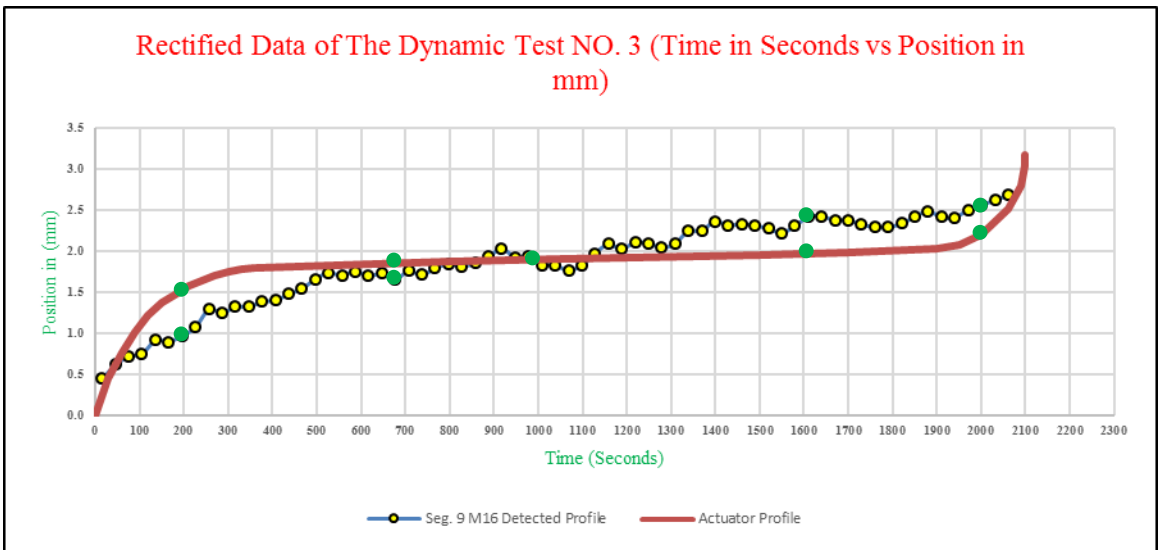


Figure 6.16: Rectified data of the dynamic test NO. 3. (The rectification including the IQR processing, Z-score processing, drift correction, simple averaging, and finally moving average).

Simply the most two things can be noticed from the test NO. 3 is the error of (vertical distance between the two green dots beside the reaction time which is half the length of each stage.

Table 6.13: Actuator vs. the detected profile of the rectified dynamic test NO. 3 data.

Test NO. 3		
Actuator Profile (mm)	Detected Profile (mm)	Absolute Precision
1.5	1	0.5
1.85	1.75	0.1
1.9	1.9	0
2	2.45	0.45
2.25	2.5	0.25

7 CONCLUSIONS AND RECOMMENDATIONS

7.1 THESIS CONCLUSIONS

One goal of the most important goals of this thesis is to validate the M16 scanner for detection the roof failure in submillimeter accuracy. It is considerable to say that the M16 detected profile after doing the outliers detection and rectification was tracking the actuator profile. In fact, it was tracking the actuator profile even with the small and slow movements and the error was in sub-millimeter as in the dynamic test NO. 2.

The steel target plate has been built and attached to a linear actuator that can move with a resolution around 0.00375 mm per step and stroke 50 mm to simulate the roof failures in mines. It was not possible to try the M16 in real mine due to the time limits and absence of not unstable mines locally, besides the intention that the author has to start with an office environment. The M16 scanner is aimed directly to target plate and collecting the displacement derived by the actuator. The results collected has many of anomalies and outliers that can be eliminated by making some of the statistical identification of outliers. All of the 16 segments in the M16 scanner is drifting together and showing very high correlation. The final results show that the M16 scanner can detect the simulated target plate profile with a precision between 0.1 mm and 3 mm per integration period.

7.2 THESIS RECOMMENDATION

The relationship between the results and the following effects should be determined more accurately:

- ❖ Zero Offset Effect
- ❖ Environmental Variables Effect such as: Noisy Environment
- ❖ Drift Effect
- ❖ M16 Settings Effect
- ❖ Segments Position Effects
- ❖ Electrical and Technological Effect
- ❖ Data Acquisition Processing and Ports and Speed of Transmitting the Data
- ❖ Speed of Transmitting the Data

- ❖ External Temperature, M16 Internal Temperature Effect
- ❖ Humidity, Dust
- ❖ Instability of the power
- ❖ Cables Type and Length
- ❖ The target plate Material Effect
- ❖ The Unknown Sources Effect

By understanding the effect of the above parameters on the collected data, it will be possible to enhance the accuracy of the M16 LIDAR. The outliers identification process has done very effective result in outlier detection. The outliers identification might need some follow-up research to apply some modern techniques that might be helpful to eliminate the anomalies such as generalized ESD (Rosner 1983). The generalized ESD is a highly recommended test for two-sided outliers identification (Iglewicz and Hoaglin 1993).

$$R_i = \max_i |x_i - \bar{x}| / \sigma \quad (7.1)$$

With \bar{x} and σ refers the sample arithmetic mean and standard deviation of the sample, respectively. Remove the observation that maximizes $|x_i - \bar{x}|$ and then recompute the above statistic with $n - 1$ measurements. The target plate should be made from a stiff material to simulate the specific fact of the roof failures. The thicker target plate might be helpful to stabilize the motion due to its heavy weight.

The internal M16 temperature could be eliminated by some of the inexpensive cooling systems such as air cooling which removes the waste heat produced by M16 scanner components and stabilize the M16 components within a permissible operating temperature window. The way of aiming the M16 to the scanned object is by using some laser spot attached to the LIDAR device. The inexpensive laser has been appended to the M16 is not very accurate and might fade with longer distance. The way of aiming the M16 toward the scanned object should also be studied to understand the relationship between the results and the angle in aiming the M16 to the scanned object, then determine the optimum angle.

BIBLIOGRAPHY

- Addison, Alonzo C. 2000. "Emerging Trends in Virtual Heritage." *IEEE Multimedia* 7 (2): 22–25.
- Addison, Alonzo C., and Marco Gaiani. 2000. "Virtualized Architectural Heritage New Tools and Techniques." *IEEE MultiMedia* 7 (2): 26–31. doi:10.1109/93.848422.
- African Consulting Surveyors. 2015. "Underground Mining Solutions." African Consulting Surveyors. <http://www.africansurveyors.com>.
- Bajpayee, T.S., Deno M. Pappas, and John L. Ellenberger. 2014. "Roof Instability." *Professional Safety* 59 (3): 57–62.
- Barrett, Steven F. 2013. *Arduino Microcontroller Processing for Everyone!: Third Edition*. 3rd ed. Morgan & Claypool Publishers.
- Berg, Brian, M. R. Mitchell, and Jim Proft. 2008. *SMST-2006: Proceedings of the International Conference on Shape Memory and Superelastic Technologies*, May 7-11, 2006, Asilomar Conference Center, Pacific Grove, California, USA. ASM International.
- Bichler, A., P. Bobrowsky, M. Best, M. Douma, J. Hunter, T. Calvert, and R. Burns. 2004. "Three-Dimensional Mapping of a Landslide Using a Multi-Geophysical Approach: The Quesnel Forks Landslide." *Landslides* 1 (1): 29–40.
- Bill Gutelius. 2014. "Review of A Low-Cost Detection and Ranging Device." *LiDAR News Magazine*, July 5. www.lidarnews.com.
- Bogdan, Laurean. 2011. "Plc as A Driver for Stepper Motor Control." *Annals of the Oradea University. Fascicle of Management and Technological Engineering* 10: 1583–0691.
- Boxall, John. 2013. *Arduino Workshop: A Hands-on Introduction with 65 Projects*. No Starch Press.
- Chen, Robert H. 2011. *Liquid Crystal Displays: Fundamental Physics and Technology*. John Wiley & Sons.
- Controls International LLC Fisher, and Emerson Process Management. 2005. *Control Valve Handbook*. 4th edition. Fisher.
- David Funkhouser. 2011. "Seismometer Puts Earthquakes Online at Kent School." December 2.

- DiBiagio, E., and O. Kjekstad. 2007. "Early Warning, Instrumentation and Monitoring Landslides 2nd Regional Training Course." RECLAIM II, 29–1.
- Dougherty, John J. 1971. "A Study of Fatal Roof Fall Accidents in Bituminous Coal Mines." Unpublished Masters Thesis, Morgantown, West Virginia: West Virginia University.
- Duong, Eric, Lyndon Shi, Eric Ward, Saurin Patel, and Aditya Sridhar. 2012. "Lidar Based Home Mapping Using the Oslrf-01 and Arduino to Generate Floor Plans."
- Eitel, Jan U. H., Lee A. Vierling, and Troy S. Magney. 2013. "A Lightweight, Low Cost Autonomously Operating Terrestrial Laser Scanner for Quantifying and Monitoring Ecosystem Structural Dynamics." *Agricultural and Forest Meteorology* 180 (October): 86–96. doi:10.1016/j.agrformet.2013.05.012.
- "Evaluation Kit and Configurator User Guide." 2015. LeddarTech Inc. www.leddartech.com.
- Frei, Erwin, Jonathan Kung, and Richard Bukowski. 2005. "High-Definition Surveying (HDS) A New Era In Reality Capture." *International Archives of Photogrammetry, Remote Sensing and Spatial Information Sciences* 36: 262–271.
- Gigli, Giovanni, Riccardo Fanti, Paolo Canuti, and Nicola Casagli. 2011. "Integration of Advanced Monitoring and Numerical Modeling Techniques for The Complete Risk Scenario Analysis of Rockslides: The Case of Mt. Beni (Florence, Italy)." *Engineering Geology* 120 (1): 48–59.
- Gopi, Satheesh, R Sathikumar, and N Madhu. 2008. *Advanced Surveying: Total Station, GIS and Remote Sensing*. New Delhi: Dorling Kindersley.
- HELM Learning Technologist. 2004. "Techniques for Exploring Data." *Helping Engineers Learn Mathematics*. April. http://www.personal.soton.ac.uk/jav/soton/HELM/helm_workbooks.html.
- Heuvel, Frank van den. 2003. *Automation in Architectural Photogrammetry: Line-Photogrammetry for the Reconstruction from Single and Multiple Images*. NCG Nederlandse Commissie voor Geodesie.
- Hoek, Evert. 2000. *Practical Rock Engineering*. North Vancouver, British Columbia Canada V7R 4H7: Rocscience Inc.
- IEWP. 2008. "The Four Elements of Effective Early Warning Systems."
- Iglewicz, Boris, and David Caster Hoaglin. 1993. *How to Detect and Handle Outliers*. ASQC Quality Press.
- John Cave. 1995. *Electromechanical Systems*. 1st ed. 10 Maltravers Street, London: The Engineering Council 1995.

- Kayal, J. R. 2008. *Microearthquake Seismology and Seismotectonics of South Asia*. Springer Science & Business Media.
- Kraus, Karl. 2007. *Photogrammetry: Geometry from Images and Laser Scans*. Walter de Gruyter.
- Leica Geosystems. 2012. "Leica FlexLine TS06 (1.5mgon) Total Station." Leica Geosystems. <http://store.leica-geosystems.us>.
- Leica Geosystems AG. 2017. "Leica ScanStation P40 / P30 - High-Definition 3D Laser Scanning Solution." Leica Geosystems. January 23.
- Louay Eldada. 2014. "Today's LiDARs and GPUs Enable Ultra-Accurate GPS-Free Navigation with Affordable SLAM." In . San Jose Convention Center: Quanergy Systems, Inc.
- Md. Khalid Hossain, Mahbubul Hoq, Mohammad Abu Sayid Haque, Md. Shah Alam, Sarwar Hossen, M. Humayun Kabir, and M. Islam. 2015. "Design and Development of a Low-Cost Microcontroller Based Liquid Crystal Display (LCD) System for Electronic Instrumentation." ResearchGate, November.
- Medina-Cetina, Zenon, and Farrokh Nadim. 2008. "Stochastic Design of Early Warning Systems." *Georisk* 2 (4): 223–236.
- Mendecki, Aleksander J., Richard A. Lynch, and Dmitriy A. Malovichko. 2010. "Routine Micro-Seismic Monitoring in Mines." In *Proceedings of Australian Earthquake Engineering Society Conference*. Perth. Western Australia: AEES 2010, Perth.
- Michoud, C., Sara Bazin, Lars Harald Blikra, Marc-Henri Derron, and M. Jaboyedoff. 2013. "Experiences from Site-Specific Landslide Early Warning Systems." <https://brage.bibsys.no/xmlui/handle/11250/2375088>.
- Milsom, John, and Asger Eriksen. 2011. *Field Geophysics*. John Wiley & Sons.
- Molinda, G. M., and Chris Mark. 2010. "Ground Failures in Coal Mines with Weak Roof." *Electron J Geotech Eng* 15: 547–588.
- Morar, Alexandru. 2011. "Four Phases Driver for Stepper Motor Control." *Scientific Bulletin of the "Petru Maior" University of Targu Mures* 8 (1): 24.
- Murphy Surveys Ltd. 2017. "3D Laser Scanning Services in UK - Murphysurveys." Blog Post. Murphy Surveys. <http://www.murphysurveys.co.uk/3d-laser-scanning/>.
- Ogundare, John Olusegun. 2015. *Precision Surveying: The Principles and Geomatics Practice*. John Wiley & Sons.

- Olsen, Michael James, John D. Raugust, and Gene Vincent Roe. 2013. Use of Advanced Geospatial Data, Tools, Technologies, and Information in Department of Transportation Projects. Transportation Research Board.
- Organizational Results Division. 2011. "New Lidar Technology Offers Faster Less Expensive Field Data." Missouri Department of Transportation.
- Oriental Motor. 2004. "EZ Limo Easy Linear Motion." Oriental Motor U.S.A. Corp. www.orientalmotor.com.
- Pappas, D. M., and C. Mark. 2012. "Roof and Rib Fall Incident Trends: A 10-Year Profile." *Transactions of Society for Mining, Metallurgy and Exploration* 330: 462–478.
- Park, Yong Tae, Pranesh Sthapit, and Jae-Young Pyun. 2009. "Smart Digital Door Lock for the Home Automation." In *TENCON 2009-2009 IEEE Region 10 Conference*, 1–6. IEEE.
- Peng, Syd S. 1978. *Coal Mine Ground Control*. 1st edition. New York: John Wiley & Sons Inc.
- Rosner, Bernard. 1983. "Percentage Points for a Generalized ESD Many-Outlier Procedure." *Technometrics* 25 (2): 165–172.
- San Jose Alonso, J. I., J. Martínez Rubio, J. J. Fernández Martín, and J. García Fernández. 2011. "Comparing Time-of-Flight and Phase-Shift. The Survey of the Royal Pantheon in the Basilica of San Isidoro (Leon)." *Int. Archives of Photogrammetry and Remote Sensing and Spatial Information Sciences* 38: 5.
- Sclater, Neil, and Nicholas P. Chironis. 2001. *Mechanisms and Mechanical Devices Sourcebook*. Vol. 3. McGraw-Hill New York.
- Sheh, Raymond, Nawid Jamali, M. Waleed Kadous, and Claude Sammut. 2006. "A Low-Cost, Compact, Lightweight 3D Range Sensor." In *Australian Conference on Robotics and Automation*.
- Shen, B., A. King, and H. Guo. 2007. "Displacement, Stress and Seismicity in Roadway Roofs During Mining-Induced Failure." *International Journal of Rock Mechanics and Mining Sciences* 45 (5): 672–88. doi:10.1016/j.ijrmms.2007.08.011.
- Sidhu, Tarlochan S., Daljit S. Ghotra, and Mohindar S. Sachdev. 2002. "An Adaptive Distance Relay and Its Performance Comparison with a Fixed Data Window Distance Relay." *IEEE Transactions on Power Delivery* 17 (3): 691–697.
- Smith, Alan D. 1984. "Mine Roof Condition and the Occurrence of Roof Falls in Coal Mines." *Proc. 2nd International Conference on Stability in Underground Mining* 84 (3): 329–345.

- Spencer, Naomi. 2014. "Two West Virginia Coal Miners Killed in Roof Collapse." World Socialist Web Site. May 14. www.wsws.org.
- Srivastava, Dhruv, Dr Ranjan, and others. 2010. "An Application-Oriented Model for Wireless Sensor Networks Integrated with Telecom Infra." arXiv Preprint arXiv:1009.1526. <http://arxiv.org/abs/1009.1526>.
- Sužiedelytė-Visockienė, Jūratė. 2013. "Accuracy Analysis of Measuring Close-Range Image Points Using Manual and Stereo Modes." *Geodesy and Cartography* 39 (1): 18–22.
- Troisi, C., and N. Negro. 2013. "Managing of EW Systems by Public Agencies Related Problems." In *Proceedings of the 1st International Workshop on Warning Criteria for Active Slides*, Courmayeur, Italy, 10–12.
- Tukey, John Wilder. 1977. *Exploratory Data Analysis*. Addison-Wesley Publishing Company.
- Uren, J., and W. F. Price. 2010. *Surveying for Engineers*. Palgrave Macmillan.
- Wyllie, Duncan C., and Chris Mah. 2004. *Rock Slope Engineering: Fourth Edition*. CRC Press.
- Zavis M , Zavodni. 2000. "Tim Dependent Movements of Open Pit Slopes." In *Slope Stability in Surface Mining*. SME.

VITA

The author, Ali Abdullah M. Alzahrani, was born in Saudi Arabia- Allith city. He received his Bachelor of Science in Geological and Environmental Engineering from King Abdulaziz University – Jeddah City – KSA, April of 2011. He received his Master’s in Geological Engineering from Missouri University of Science and Technology – Rolla City - MO 65409 – USA, December of 2017. The author has taught the lab portion of Rock Mechanics, Rock in construction, Application in Geological Engineering and Soil Mechanics under the guidance of a group of professors at King Abdulaziz University.

The author has published one book in the Arabic Language under the social development field which has been distributed in All Arabic countries.

The author published one paper that it explored the protective dams in the eastern region of Jeddah City- Saudia Arabia after the catastrophic floods which destroyed the infrastructure of the city. The recommendation of this paper has matched the safety standards which are required for these types of dams.

After two years the author started communicating with Dr.Norbert Maerz in MST to continue his higher education in Geological Engineering. The author began working on his master’s degree in Geological Engineering at Missouri S&T, working under Dr.Norbert Maerz in late 2014.

The author worked as a Graduate Research Assistant, where he worked on using TerraTek for various projects such as (Stress-Strain Relationship – Uniaxial Compression Test – Triaxial Test “Hoek Cell”) besides working on the M16 Leddar Evaluation Kit.